DISSERTATIONES
CHIMICAE
UNIVERSITATIS
TARTUENSIS
223

ERNESTO DE JESUS ZAPATA FLORES

Derivatization Reagents used in negative mode electrospray LC-MS

DISSERTATIONES CHIMICAE UNIVERSITATIS TARTUENSIS
223

DISSERTATIONES CHIMICAE UNIVERSITATIS TARTUENSIS
223

ERNESTO DE JESUS ZAPATA FLORES

Derivatization Reagents used in negative mode electrospray LC-MS

UNIVERSITY OF TARTU
Press
1632

Institute of Chemistry, Faculty of Science and Technology, University of Tartu, Estonia.

The dissertation is accepted for the commencement of the degree of *Doctor Philosophiae* in Chemistry on June 22, 2023 by the Council of Institute of Chemistry, Faculty of Science and Technology, University of Tartu.

Supervisors: Associate Professor Koit Herodes
Institute of Chemistry, University of Tartu, Estonia

Professor Ivo Leito
Institute of Chemistry, University of Tartu, Estonia

Opponent: Associate Professor Jeffrey Hawkes
Department of Chemistry – BMC, University of Uppsala, Sweden.

Commencement: 30th August 2023, at 10:15, Auditorium 1020, Chemicum, Ravila 14a, Tartu

ISSN 1406-0299 (print) ISSN 2806-2159 (pdf)
ISBN 978-9916-27-290-9 (print) ISBN 978-9916-27-291-6 (pdf)

University of Tartu Press
www.tyk.ee

TABLE OF CONTENTS

LIST OF ORIGINAL PUBLICATIONS

1. **Zapata Flores, E. de J**.; Herodes, K.; Leito, I. Comparison of the Ionisation Mode in the Determination of Free Amino Acids in Beers by Liquid Chromatography Tandem Mass Spectrometry. *Journal of Chromatography A* **2022**, *1677*, 463320. https://doi.org/10.1016/j.chroma.2022.463320.

2. **Zapata Flores, E. de J**.; Bùi, N. K. N.; Selberg, S.; Herodes, K.; Leito, I. Comparison of Two Azobenzene-Based Amino Acid Derivatization Reagents for LC-MS/MS Analysis in Positive and Negative ESI Modes. *Talanta* **2023**, *252*, 123803. https://doi.org/10.1016/j.talanta.2022.123803.

3. **Zapata E,** Leito I, Herodes K. Positive + negative is not equal to zero: Use of negative ionisation as analyte identity confirmation tool in LC-ESI-MS analysis. European Journal of Mass Spectrometry. 2022;28(5-6):107-112. doi:10.1177/14690667221130160.

Author's contribution

Paper I: The main person responsible for planning and performing the experiments, data treatment and writing the manuscript.

Paper II: The main person responsible for planning and performing the quantitation experiments and writing the manuscript.

Paper III: The main person responsible performing the experiments, data treatment and writing the manuscript.

ABREVIATIONS

MeCN	Acetonitrile
AcMe	Acetone
ESI-MS	Electrospray mass spectrometry
FA	Formic Acid
HAcO	Acetic Acid
HPLC	High Performance Liquid Chromatography
LC	Liquid Chromatography
LoD	Limit of Detection
LoQ	Limit of Quantitation
m/z	Mass to charge ratio
MeOH	Methanol
MS	Mass spectrometry
UHPLC	Ultra-high pressure liquid chromatography
DEEMM	Diethyl ethoxymethylenemalonate
AzoB	Azobenzene N-hydroxysuccinimidyl carbamate
AzoC	4-(phenylazo)benzoic acid N-succinimidyl ester
NLS	Neutral Loss Scan
MS/MS	Tandem mass spectrometry
APPI	Atmospheric Pressure Photoionization
APCI	Atmospheric Pressure Chemical Ionization

1. INTRODUCTION

Liquid chromatography (LC) is one of the most widespread analytical techniques, it allows to separate the analytes from potential interferents and from each other. When it is coupled with mass spectrometry (MS), it becomes a powerful technique, that permits not only the separation but also the identification and quantification of the analytes at very low concentration levels.

Due to the vast diversity of analytes and matrices, LC-MS is susceptible to several factors. The retention of the analytes on the stationary phase must be such that it allows a good separation, while at the same time, they should be easily ionizable in the ionization source. It is often difficult to simultaneously meet both conditions. Added to these phenomena, the matrix effect – suppression/enhancement of analyte's ionization by co-eluting compounds – is one of the biggest disadvantages that affect LC-MS analysis. There are different approaches to overcome this problem. One of them is the derivatization of the analytes. Its role is not only to improve chromatographic retention, but also to increase the ionization efficiency which is translated into low limits of detection (LoD) and quantification (LoQ). Better retention (less co-eluting substances) together with better ionization efficiency (reducing the effect of co-eluters on ionization) both lead to reducing matrix effects.

Among different substances that are analyzed in reversed-phase liquid chromatography (RP-LC), amino acids are among the most challenging analytes. Because of their high polarity, the direct analysis in RP- LC is problematic due to low retention. Despite being highly polar, their ionization efficiencies in the electrospray source are low.

Because of the nature of the current derivatization reagents, the analysis of their derivatives has been carried out mainly in positive ionization mode, leaving the negative ionization mode aside.

The aim of this work is to show some of the benefits of the negative ionization mode in LC-MS/MS analysis of amino compounds, focusing on amino acids: Different derivatization, both commercial and newly developed, were used for the analysis of amino acids in different drinks. Both positive and negative modes, as well as their combination were used.

2. LITERATURE REVIEW

2.1 LC-MS/MS

Liquid chromatography (LC) had its origins around 1940 and 1950 [1], [2], it has grown and developed by leaps and bounds during the last decades, to become one the most popular analytical techniques around the globe. One of the reasons of its popularity is the fact that, it can be used with several detectors such as UV, fluorescence, refractive index, conductivity, just to name a few. However, when it is coupled to mass spectrometry (MS) it becomes one of the most powerful techniques that allows to detect and quantify a highly diverse range of substances at low trace levels in a vast variety of samples. To illustrate its usefulness, searching articles published during the last five years (2018-2022) that contain the term "LC-MS" or "liquid chromatography tandem mass spectrometry" on their title, the Web of science search engine returns more than 6000 results. This shows the popularity as well as the utility and versatility of this technique, in disciplines ranging from toxicology, veterinary sciences, medicine legal, to analytical chemistry.

Among the different ionization sources used in LC-MS, electrospray ionization (ESI), developed by John Fenn in the 80's [3], is currently the most commonly used. It enables soft ionization that allows to convert the dissolved analyte into the gas phase without modifying its molecular structure [4]. Another advantage of ESI over other soft ionization sources such as APPI and APCI are the low limits of detection that can be reached as well as higher S/N ratios [5].

Tandem mass spectrometry (MS/MS) was developed to increase the specificity of the analysis even further once the chromatographic separation has been reached. There are several mass analyzers to perform MS/MS analysis, for example quadrupole-time of flight (Q-ToF), ion trap or triple quadrupole (QqQ). In this work, MS/MS analysis were performed using triple quadrupole instruments since they allow to improve the signal-to-noise ratio (S/N) [6], the reproducibility and achieve lower detection and quantification limits compared to the single quadrupole mass spectrometer.

As stated by its name, QqQ consists of a series of three quadrupoles. The first one works as a mass filter that allows the passage of the ions (so-called precursor or parent ions) of interest, discarding all other ions produced in the ionization source. In the second quadrupole (collision cell), the precursor ions are given additional kinetic energy by applying an electrical potential and then they collide with a neutral gas (N_2, He or Ar). Finally, after fragmentation, ions are directed to the third quadrupole where they are scanned depending on the selected scan mode (product ion, precursor ion, neutral loss, MRM, etc.). Figure 1 illustrates the functioning of QqQ.

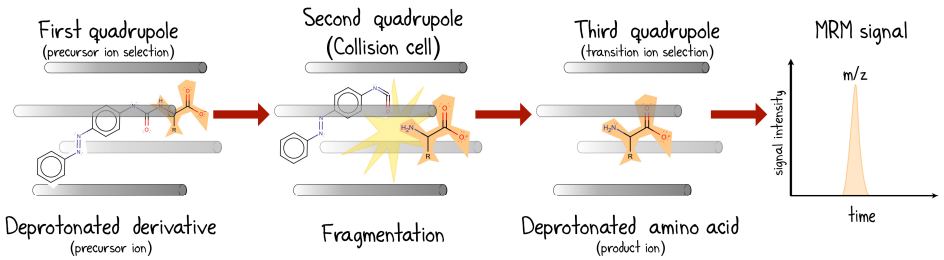

Figure 1. Example of fragmentation in a triple quadrupole instrument.

2.2 Amino acid analysis

Amino acids (AAs) are well known substances, there are several hundreds of them in the nature. The 20 proteinogenic amino acids are the "building blocks" for synthesizing the proteins and are genetically encoded in the DNA. The remaining amino acids are called non-proteinogenic amino acids and they also have important roles in different processes in the living beings. As examples, gamma aminobutyric acid (GABA) acts as neurotransmitter [7]; L-homocysteine is found in the blood and depending on its levels, has been associated to heart diseases [8], [9]; L-3,4-dihidroxyphenylalanine (L-DOPA) and L-Canavanine are used by some plants as toxins against predators [10], [11]. Figure 2 presents the structures amino acids used in this project.

The determination of AAs is very important, due to their vast variety of applications. For example: in the pharmaceutical industry, AAs are used as ingredients in some formulations to improve their properties [12], [13]; in the medical field they are used as diagnosis tool to identify metabolic disorders [14]; in food industry despite being essential nutrients, amino acids are used as foods additives, e.g. glutamic acid salts (sodium, potassium, etc.) [15]. Amino acids can be used as markers to prevent adulteration [16] or to determine geographical origin of certain foods [17], [18]. The intake of amino acids as efficiency training enhancers for athletes has also been studied [19], [20].

Depending on the structure of amino acids, they can be classified in aliphatic, aromatic (Phe and Tyr), imino (Pro and Hyp), and heterocyclic (Trp and His) amino acids. Another classification is based on their polarities: those with non-polar side-chains (Gly, Ala, Val, Leu, Ile, Met, Phe, Trp and Pro), with polar chains (Ser, Thr, Tyr, Asn, Gln) as well as amino acids with charged side chains (Asp, Glu, His, Lys, Arg).

The fact that amino acids contain a basic amino group as well as an acidic carboxylic group in the same molecule makes difficult their direct analysis using LC-MS. Due to their high polarities, their retention on the stationary phase is poor and besides the retention issue, just as problematic is the typically poor ionization efficiency they have [21] To overcome this problem, derivatization is frequently applied to improve their chromatographic behavior as well as their detection which is translated into obtaining better and more reliable results.

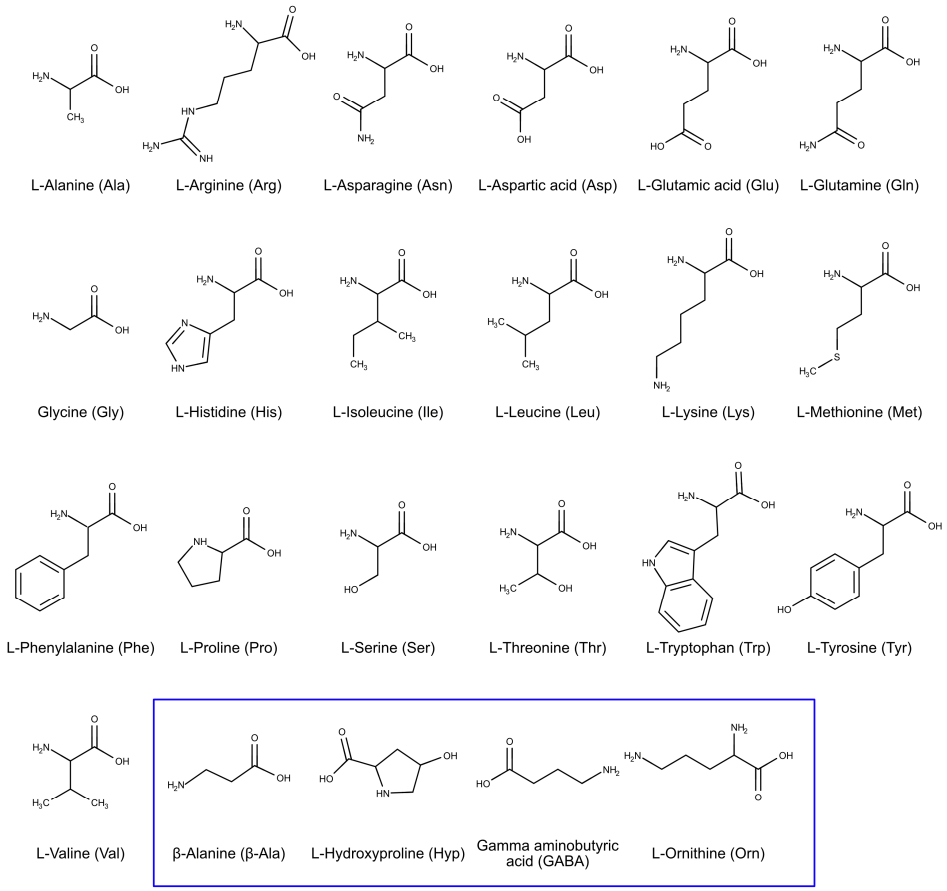

Figure 2. Structure of the amino acids used in this work. Inside blue box, non-proteinogenic amino acids.

2.3 Derivatization reagents for amino acids in LC and LC-MS

There are several examples (Figure 3) of derivatization reagents that have been used in the analysis of amines and amino acids, such as o-Phthalaldehyde (OPA) [22]; ninhydrin [23], phenylisothiocyanate (PITC) [24], [25], 6-aminoquinolyl-N-hydroxy-succinimidyl carbamate (AQC) [26], [27], diethyl ethoxymethylenemalonate (DEEMM) [28], [29], 5-(dimethylamino)naphthalene-1-sulfonyl chloride (Dansyl-Cl) [30], etc.

These reagents were originally meant to be used with UV-Vis or fluorescence detection, and a few of them have been successfully used with ESI-MS detection, for example, Dansyl-Cl [31], AQC [27] and DEEMM [29], [32]. Dansyl-Cl and AQC work well in positive ionization mode since they contain nitrogen that acts as protonation center.

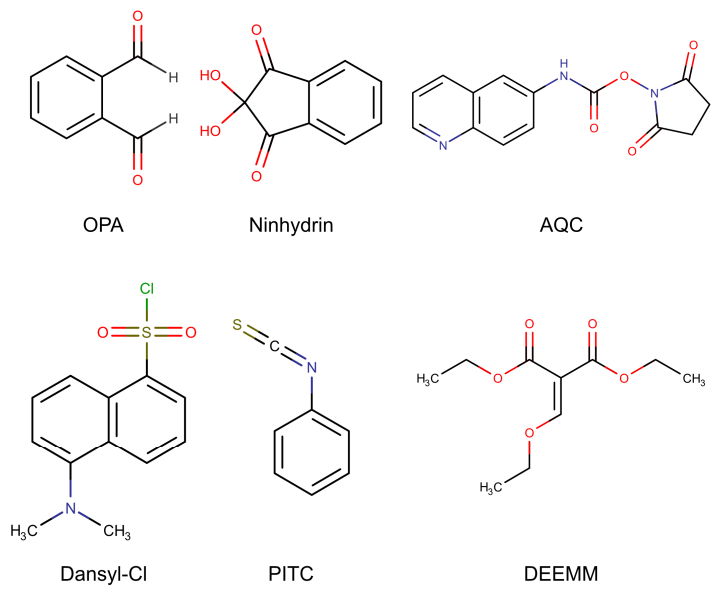

Figure 3. Structures of derivatization reagents used for the analysis of amino compounds.

However, those derivatization reagents are not free from disadvantages. For example, OPA is not able to react with secondary amines [33] (therefore, proline and hydroxyproline cannot be analyzed) and its derivatives are not very stable [34]. In case of DEEMM, its main concern is the fact that it requires 24 h to react completely with proline [29]. Ninhydrin color yield is affected by the presence of more than one amino group, lysine or other diamino acids, must have one of their amino groups acetylated to produce normal color yield [35].In case of Dansyl-Cl, pH control is very important since high pH favors the conversion of Dansyl-Cl to dansyl sulfonic acid which affect the derivatization yield because this conversion competes with the derivatization reaction, additionally, if a large excess of Dansyl-Cl is present, it can react with the derivatized amino acids, producing several side products [30]. The separation of AQC derivatives depends to a great extent on the column temperature and pH of the eluent [36], in addition, AQC-tryptophan derivative shows a low response to fluorometric detection and AQC-cysteine derivative is poorly detected [27].

In the last decades, due to the increasing use of mass spectrometric detectors, new derivatization reagents designed specifically for LC-ESI-MS/MS (Figure 4) have been developed, including p-N,N,N-trimethylammonioanilyl N'-hydroxysuccinimidyl carbamate iodide (TAHS) [37], [38], (5-N-succinimidoxy-5-oxopentyl)triphenylphosphonium bromide (SPTPP) [39], [40], 3-aminopyridyl-N-hydroxysuccinimidyl carbamate (APDS) [41] and dibenzyl ethoxymethylene malonate (DBEEMM) that was developed in our research group [42].

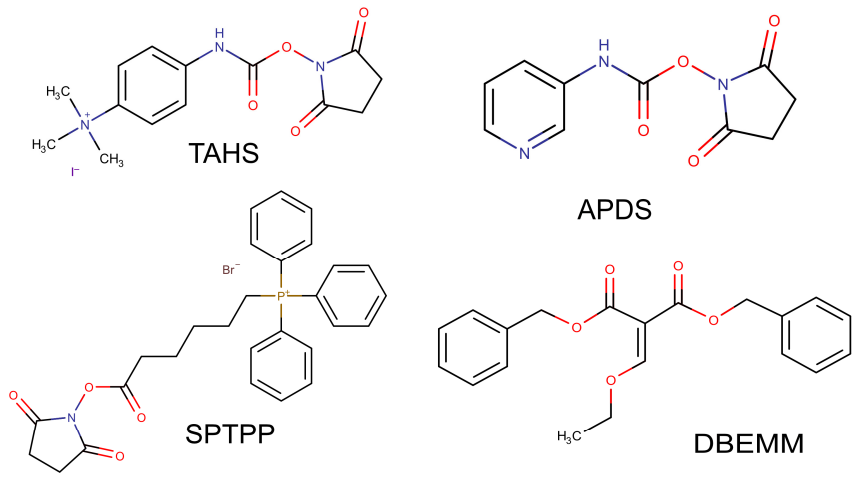

Figure 4. Derivatization reagents synthesized for LC-MS/MS.

From these reagents, TAHS and SPTPP are permanently charged positively which improves their ionization efficiency and allows to reach a very high sensitivity (lower limits of detection), however, because of being permanently charged and therefore highly polar, the separation of TAHS derivatives in reversed phase LC is difficult [41]. Since TAHS and SPTPP are positively charged, their use is restricted to positive ESI.

Usually LC-MS analysis is done in positive ionization mode leaving negative ionization aside, because most of the analytes ionize well in ESI(+), however, compounds present in the matrix, can also ionize affecting the analysis by suppressing or enhancing the signals of the analytes [43]–[46]. In addition, the formation of adducts is more common in positive than in negative mode [47]. For example, it has been reported that sodium adducts can fragment poorly in MS [48]. Thus, negative ion mode might be convenient in some cases since it can produce spectra with less background noise [49] and it is less affected to matrix effects [50], [51].

For negative ESI, the derivatization reagents should fulfill the condition of incorporating groups that facilitate the ionization, such as sulfonic or carboxylic acid groups. For example, Ns-MOK-β-Pro-OSu (2,5-dioxopyrrolidin-1-yl(4-(((2-nitrophenyl)sulfonyl)oxy)-6-(3-oxomorpholino)quinoline-2-carbonyl)-pyrrolidine-3-carboxylate), whose derivatives can be detected in negative mode because they produce the nosylate moiety fragment (202 m/z) [52]. However, since amino acids themselves contain the carboxylic acid moiety, the previous condition is not mandatory, and simpler reagents such as Fmoc-Cl (9-fluorenylmethoxycarbonyl chloride), have been used to analyze amino acids in negative mode [48].

In this work, besides DEEMM, two more derivatization reagents (Figure 5) were investigated, Azobenzene N-hydroxysuccinimidyl carbamate (named in

this work as “AzoB”, because of azobenzene), that was previously studied by Strydom using LC-UV in 1996 [53], and AzoC, (4-(phenylazo)benzoic acid N-succinimidyl ester), whose use was restricted mainly to photochemistry [54], [55], but their application to LC-MS/MS analysis, was never been explored before.

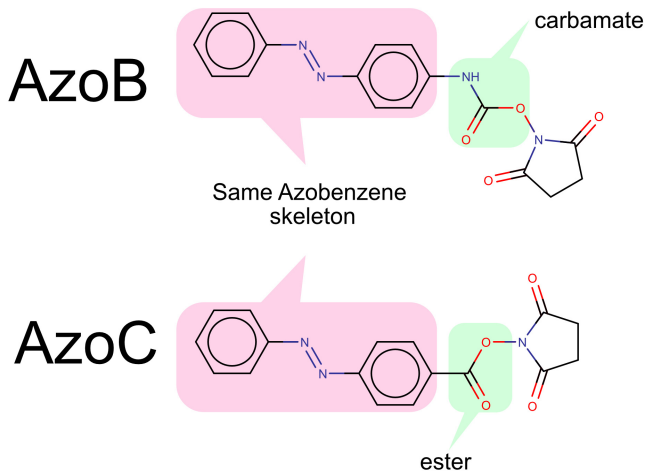

Figure 5. Structures of AzoB and AzoC, their similarities and differences are presented.

2.4 Identity confirmation in LC-MS

Misidentifying compounds is one of the most critical errors during a chemical analysis, therefore the correct identification of analytes is very important to provide reliable results. In LC, the first step that tentatively allows to identify a compound is the comparison of the retention time of the peak of the analyte in a standard solution against the peak in the sample solution. However, finding two different substances sharing the same retention time is not a rare situation. Therefore, just matching retention time is not a statement strong enough to ensure that peak in sample solution corresponds to the analyte. It is where tandem MS outshines other detectors used in LC. First, MS allows identifying the analyte because of the mass to charge ratio (m/z) of its ionized form (precursor ion), and, to go one step further, by its fragmentation pattern, i.e. the product ions formed upon fragmentation.

Among the different validation guidelines applicable to identity confirmation of analytes, there are two that address LC-MS/MS in particular: SANTE/11312/2021 [56] and 2021/808 (that replaced 2002/657/EC) [57]. The former establishes that to carry out a quantitative analysis using LC-MS/MS and ensure the identity of the analyte accurately, a minimum of two product ions have to be obtained for each analyte [56] the so-called quantifier and qualifier (or identifier) ions. The quantifier ion is the one that produces the peak with the

maximum height or area, this ion is used to estimate the concentration of the analyte from the calibration curve. While the qualifier ion is used as an additional information source to confirm the identity of the analyte.

The 2021/808 guideline has a stricter system of identification points that depends on the type of the analyte. In case of analysis of authorized substances, which have an established maximum residue limit at least 4 identification points must be obtained, while for unauthorized or prohibited substances, 5 points are required, for example using LC-MS/MS where 2 product ions are recorded, 5 points are obtained (1 point from LC separation, 1 point from precursor ion and 1.5 from each of the two different product ions) [57].

Quantifier and qualifier ions are typically obtained from the same ionization mode, nonetheless, there are cases in which one polarity does not provide enough transitions. In paper III, an alternative approach is presented, the usage of transitions obtained in positive mode as quantifier transitions and transitions in negative mode as qualifier transitions. The evaluation was carried out according to the SANTE/11312/2021 and 2021/808 guidelines.

3. EXPERIMENTAL

3.1 Chemicals and preparation of standard solutions

Standard solutions of amino acids (paper I to III) and biogenic amines (paper II) were prepared as stated in their respective manuscripts, in all cases LC-MS grade chemicals were used unless expressed otherwise.

3.2 Samples and sample preparation

Beer samples (Paper I): 15 beer samples were purchased from local grocery stores; the beers were classified in two main groups mass-produced and hand-crafted beers. The first group included local (Estonian) as well as other European brands while second group was merely formed by Estonian handcrafted beers.

For sample treatment, a simple approach was followed, beers were degasified by sonication for 20 minutes, samples were diluted using 0.1 mol L^{-1} HCl containing 30% MeOH. Typical dilution factors ranged from 1:100 up to 1:1000. HCl was used as preserving agent to protect analytes from degradation as well as to keep amino acids in their protonated forms.

Kali and juice samples (Papers II and III): Four samples of Kali as well as tomato juice were purchased from local grocery stores, while watermelon juice was freshly prepared in the lab. Samples of Kali were sonicated for 15 min, after that, they were filtered and diluted 25 times with 0.1 mol L^{-1} HCl. Watermelon and tomato juices were centrifuged for 10 min at 7500 rpm, 1 mL of filtered supernatant of each juice was diluted with hydrochloric acid (dilutions factors ranged from 100 to 2000).

3.3 Derivatization procedures

DEEMM (Paper I): 250 µL of sample or standard solution were placed into a vial. 875 µL of borate buffer (0.75 mol L^{-1}, pH 9) and 375 µL of DEEMM solution (1:50 in MeOH) were added. Vials were vortexed for 1 minute and kept protected from direct light at room temperature. Analysis was performed 24 h after the derivatization. Before injecting, derivatized samples, were filtered through regenerated cellulose syringe filters with pore size of 0.2 µm. Derivatization reaction is presented in Figure 6.

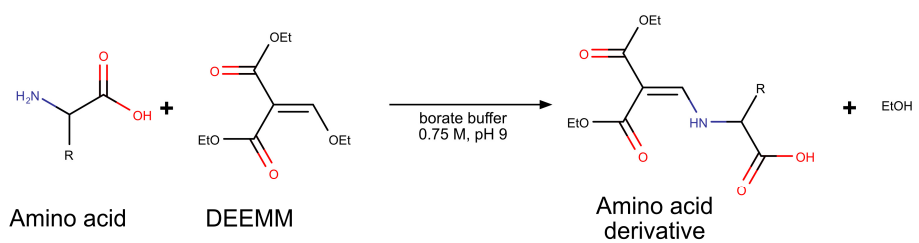

Figure 6. Reaction between amino acids and DEEMM.

AzoB and AzoC (Papers II and III): 90 µL of 0.5 mol L^{-1} borate buffer (pH 9) were pipetted into a 2 mL Eppendorf microtube, 40 µL of sample (or standard) solution were added and the vial was vortexed for 30 seconds. Thereafter 70 µL (120 µL in case of AzoC) of the derivatization reagent solution were added (2000 µg mL^{-1} in MeCN). This mixture was vortexed for 30 s and then heated at 50 °C for 5 min. After this, vials were let to rest for 5 min, followed by the addition of 400 µL (350 µL in case of AzoC) of 0.2% acetic acid in a mixture MeCN-water (1:1 v/v) to quench the reaction. Before being injected into LC-MS, derivatized samples were filtered through regenerated cellulose syringe filters pore size of 0.2 µm. Derivatization reactions are shown in Figure 7 for AzoB and Figure 8 for AzoC.

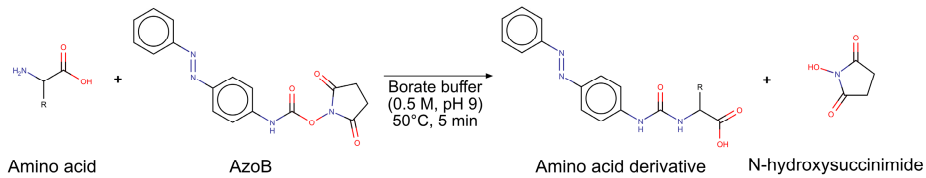

Figure 7. Derivatization of amino acids with AzoB to form disubstituted ureas.

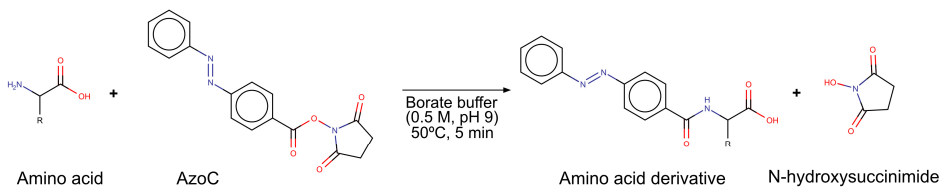

Figure 8. Derivatization reaction of amino acids with AzoC to produce amides.

3.4 LC-ESI-MS/MS analysis

In this work three different instruments were used. One with single quadrupole mass and the other two with triple quadrupole (QqQ) mass analyzer. The operational parameters are presented below:

Single quadrupole instrument for ionization efficiency measurements: Shimadzu Nexera X2 UHPLC coupled to LCMS-2020 mass spectrometer. Interface temperature 350 °C, desolvation line (DL) temperature 290 °C, DL voltage 0 V, heat block temperature 350 °C, drying gas flow 20 L min^{-1}. Eluent flow rate 0.2 mL min^{-1}.

Triple quadrupole (QqQ) instrument in paper I: LC-ESI-MS/MS system, Agilent 1290 UHPLC coupled to Agilent 6495 Triple Quad LC/MS with Jet Stream ion source. Nebulizer gas pressure 40 psi, drying gas (N_2) flow rate 11 L min^{-1} and temperature 235 °C, sheath gas temperature 400 °C and flow rate 12 L min^{-1}, capillary voltage 3500 V for both ionization modes, nozzle voltage for

positive mode 500 V and -1500 V for negative mode. iFunnel parameters: High pressure RF for both modes 130 V, low pressure RF for positive mode 60 V and 80 V for negative mode.

Triple quadrupole instrument in papers II and III: LC-ESI-MS/MS system, Agilent 1260 UHPLC coupled to Agilent 6460 Triple Quad LC/MS with Jet Stream ion source. MS parameters: Drying gas (N_2) temperature: 350 °C and flow rate: 13 L min^{-1}; Nebulizer pressure: 40 psi; Sheath gas temperature: 350 °C and flow rate: 12 L min^{-1}. Capillary voltage for both polarities: 3500 V and Nozzle Voltage:1000 V for both polarities.

Table 1 presents the different chromatographic methods used in this work.

Table 2 presents the retention times and MS parameters for DEEMM amino acid derivatives.

Table 3 presents the retention times, molecular weights, and MS parameters for AzoB amino acid derivatives.

Table 4 presents the retention times, molecular weights, and MS parameters for AzoC amino acid derivatives.

Table 1. Chromatographic methods for the analysis of amino acid derivatives.

	Paper I	Paper II, III	Paper II
	DEEMM	AzoB	AzoC
Instrument	LC-ESI-MS/MS system, Agilent 1290 UHPLC coupled to Agilent 6495 Triple Quad LC/MS	LC-ESI-MS/MS system, Agilent 1260 Infinity II UHPLC coupled to Agilent 6460 Triple Quad LC/MS	
Column	C18 ZORBAX RRHD (2.1 ×50 mm, 1.8 µm) ZORBAX Eclipse Plus C18 guard column (2.1 ×5 mm, 1.8 µm).	Biphenyl column (Kinetex 50 × 2.1 mm, 1.7 µm). Biphenyl guard column (Phenomenex 2.1 mm)	
Eluent composition	A: 0.1% aqueous formic acid B: Acetonitrile (4%H_2O)	A: 0.1% aqueous formic acid B: Methanol	
Flow Rate	0.4 mL min^{-1}		
Gradient (%B)	0-1 min 10%, 1-1.5 min, 10-15% 1.5-4.5 min, 15% 4.5-6.5 min, 15-35% 6.5-12 min, 35% 12-13 min 35-100% 13-16 min, 100% 16-17 min, 100-10%	0–2 min 45% 2–11 min 45–83% 11–12 min 83–100% 12–16 min 100% 16–17 min 100-45%	
Post time	6 min	3 min	
Injection volume	2 µL		

Table 2. Retention times, collision energies (CE) and transitions for DEEMM amino acid derivatives in both ionization modes (Paper I).

Derivative	Retention time (min)	Derivative nominal mass (g mol^{-1})	Positive mode			Negative mode		
			Precursor $[M+H]^+$	Product, m/z	CE (V)	Precursor $[M-H]^-$	Product, m/z	CE (V)
HIS	1.71	325	326	280	6	324	234	13
ARG	2.40	344	345	299	10	343	257	16
ASN	2.69	302	303	257	10	301	257	9
GLN	3.00	316	317	271	10	315	271	9
SER	3.21	275	276	230	10	274	212	9
ASP	3.85	303	304	258	10	302	258	9
GLY	4.71	245	246	200	10	244	154	9
GLU	4.75	317	318	272	10	316	226	9
THR	4.94	289	290	244	10	288	226	9
β-ALA	5.82	259	260	214	6	258	186	13
GABA	6.364	273	274	228	6	272	186	17
α-ALA	6.51	259	260	214	10	258	214	8
PRO	6.56	285	286	240	8	284	194	9
TYR	6.98	351	352	306	6	350	306	9
MET	7.80	319	320	274	8	318	274	9
VAL	8.03	287	288	242	10	286	242	9
TRP	8.75	374	375	329	8	373	283	13
ORN*	9.20	472	473	427	4	471	427	13
ILE	9.62	301	302	256	10	300	256	9
LEU	9.92	301	302	256	10	300	256	9
PHE	9.38	335	336	290	10	334	290	9
LYS*,$^{++}$	10.49	486	509^{++}	463	18	485	441	13
*amino acid reacted with 2 molecules of DEEMM								
$^{++}$sodium adduct								

Table 3. Retention times, precursor, and product ions as well as collision energy voltages (CE) and fragmentor voltages used for AzoB amino acid derivatives (Papers II and III).

Amino acid derivative	Retention time (min)	AzoB derivative nominal mass (g mol^{-1})	ESI+ MRM				ESI- MRM			
			Precursor ion (m/z)	Product ion (m/z)	CE (V)	Fragmentor (V)	Precursor ion (m/z)	Product ion (m/z)	CE (V)	Fragmentor (V)
His	2.8	378	379	224	16	110	377	154	12	117
Arg	3.1	397	398	201	16	110	396	173	8	117
HyPro	4.0	354	355	224	16	135	353	130	12	85
Asn	4.6	355	356	224	16	120	354	131	8	110
Gln	4.7	369	370	224	16	110	368	145	12	110
Ser	5.1	328	329	224	12	135	327	104	12	135
Gly	5.4	298	299	224	4	114	297	100	4	114
Asp	5.6	356	357	224	12	85	355	132	8	85
Glu	5.7	370	371	224	12	85	369	146	12	85
Thr	6.0	342	343	224	12	135	341	118	8	118
β-Ala	6.2	312	313	224	10	135	311	88	8	110
α-Ala	6.4	312	313	224	10	135	311	88	8	110
GABA	6.5	326	327	224	12	120	325	102	4	135
Pro	7.2	338	339	224	16	110	337	114	20	114
Tyr	7.6	404	405	224	16	110	403	180	12	113
Val	8.0	340	341	224	12	135	339	116	8	60
Met	8.4	372	373	224	16	110	371	148	8	114
Leu-Ile	8.8	354	355	224	16	110	353	130	8	117
Trp	9.3	427	428	188	16	110	426	203	8	114
Phe	9.5	388	389	224	16	110	387	164	12	117
Orn*	11.5	578	579	224	16	135	577	354	12	113
Lys*	11.7	592	593	224	20	135	591	368	12	132
*Disubstituted derivatives										

Table 4. Retention times, precursor, and product ions as well as collision energy voltages (CE) and fragmentor voltages used for AzoC amino acid derivatives (Paper II).

Amino acid derivative	Retention time (min)	AzoC derivative nominal mass (g mol^{-1})	ESI+ MRM				ESI- MRM			
			Precursor ion (m/z)	Product ion (m/z)	CE (V)	Fragmentor (V)	Precursor ion (m/z)	Product ion (m/z)	CE (V)	Fragmentor (V)
His	2.4	363	364	209	24	120	362	318	12	98
Arg	2.7	382	383	209	32	120	381	295	20	98
Asn	4.3	340	341	209	20	120	339	295	8	120
Gln	4.5	354	355	209	20	120	353	291	12	120
Hyp	4.7	339	340	209	16	98	338	266	8	120
Ser	4.9	313	314	209	12	120	312	250	8	120
Asp	5.3	341	342	209	20	76	340	224	16	98
Gly	5.3	283	284	209	12	120	282	210	8	98
Glu	5.6	355	356	209	8	76	354	310	12	76
Thr	5.9	327	328	209	12	120	326	264	12	120
α-Ala	6.4	297	298	209	12	98	296	252	12	120
GABA	6.6	311	312	209	12	76	310	181	20	120
Tyr	7.4	389	390	209	20	98	388	344	8	98
Val	8.3	325	326	209	12	120	324	209	12	120
Pro	8.5	323	324	209	8	120	322	250	8	98
Met	8.6	357	358	209	12	120	356	284	8	120
Leu	8.9	339	340	209	16	98	338	209	16	98
Ile	9.1	339	340	209	16	98	338	209	16	98
Trp	9.6	412	413	209	20	120	411	209	16	120
Phe	9.7	373	374	209	12	120	372	209	12	120
Lys*	11.8	561	563	209	36	120	561	517	20	120
Orn*	11.8	548	549	209	32	98	547	503	20	120
*Disubstituted derivatives										

4. RESULTS AND DISCUSSION

All studied derivatization reagents (DEEMM, AzoB and AzoC) can be used both in positive and negative ionization mode. However, the transition patterns for DEEMM and AzoC derivatives in negative mode are more complex than their counterparts in positive mode. This contrasts with the amino acid derivatives of AzoB that have well defined fragmentation patterns in both ionization modes. This phenomenon will be explained in more detail in section 4.1.3.

4.1 Method development

To obtain reliable results from an analytical method involving derivatization, there are two main factors to be considered. Firstly, the derivatization process needs to be optimized and validated. Secondly, the different LC-ESI-MS parameters need to be properly evaluated and optimized to reach the highest sensitivity. Therefore, before carrying out the analysis of samples, the chromatographic separation, derivatization yield, ion source and mass spectrometric parameters were evaluated and optimized.

4.1.1 Optimization of derivatization procedures

DEEMM derivatization has been carried out in our research group before [29], [58] and its derivatization procedure was optimized already. However, in case of AzoB and AzoC (Paper II and III) because their use as derivatization reagents for LC-ESI-MS/MS is new, their derivatization procedures needed to be optimized.

Optimization of AzoB and AzoC derivatization: Samples and standard solutions were initially diluted in 0.1 mol L^{-1} HCl. Therefore, all amino acids were in the solution in their protonated forms and were unable to react with the derivatization reagents. Thus, a basic medium was required. Different derivatization reaction conditions were tested (buffer concentration, reaction time and effect of temperature) to observe their impact on the peak area of the derivatives of AzoB, once this optimization was carried out, it was found that same conditions were also suitable for derivatization with AzoC. Borate buffer concentration ranged from 0.25 to 0.75 mol L^{-1} (all of them kept at pH 9), while derivatization was carried out at room temperature (20 °C) and at 50 °C; reaction times were set to 5, 15 and 30 minutes. Optimal derivatization procedure for both reagents is summarized in experimental section 3.3.

AzoB and AzoC derivatives of Gly, Pro and Phe were synthesized specifically for evaluating the yield of derivatization, those amino acids were selected based on their structures: glycine is the simplest amino acid, it was expected it would react faster than more complex molecules, such as proline (secondary amine) or phenylalanine (possibly affected by steric effect). To avoid any influence of matrix effect, the synthesis was done in solution without

any matrix, yields were assessed using LC with UV detector. The observed derivatization yields were close to 100 % for the three AzoB derivatives. With AzoC the derivatization of glycine was close to 100% but for proline and phenylalanine the yield was less than 90%.

4.1.2 Optimization of chromatographic analysis

Theoretically, when dynamic multiple reaction monitoring (dMRM) is used, given that specific transitions are used, a perfect chromatographic separation is no longer required. However, usually samples contain other substances that can coelute with the analytes causing signal suppression or enhancement. Therefore, to minimize the impact of this phenomenon it is still important to achieve a good chromatographic separation.

In case of DEEMM (paper I) the usage of formic acid and acetonitrile with the traditional C18 column provided enough separation with only few overlapping peaks. In the case of AzoB derivatives (paper II and III) methanol as the organic eluent component and a biphenyl column offered a better separation of peaks than the C18 stationary phase (Figure 9).

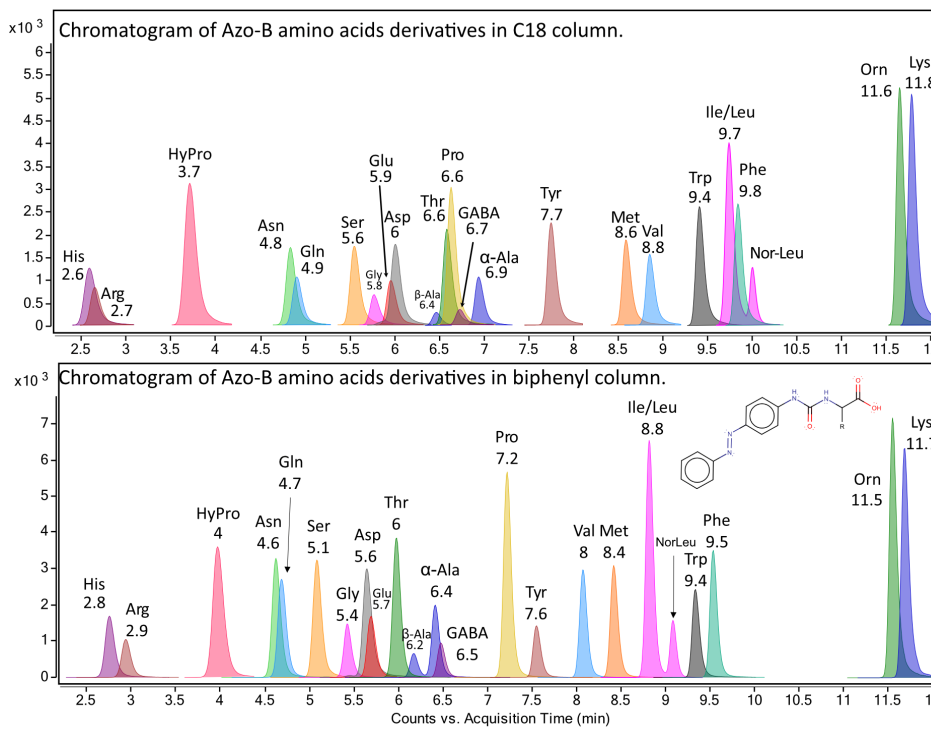

Figure 9. Comparison of AzoB derivatives behavior in C18 column (top) and biphenyl column (bottom) under the same gradient conditions; same derivatives share same color to make comparison easier.

Because of the similarity between AzoB and AzoC structure (azobenzene moiety), the derivatives of both derivatization reagents have comparable chromatographic behavior; however, in the case of AzoC derivatives, leucine and isoleucine are only partly coeluting, unlike AzoB derivative where they elute together (Figure 10).

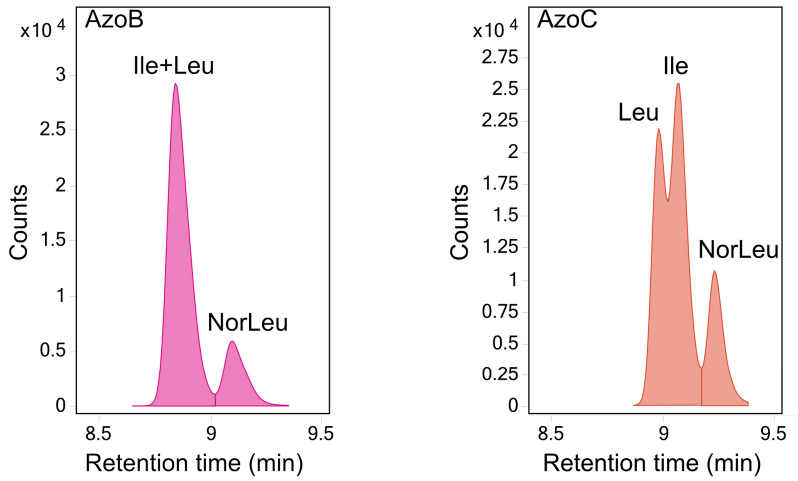

Figure 10. Comparison of the behavior of AzoB and AzoC leucine and isoleucine derivatives.

4.1.3 MS behavior (Papers I and II)

When new derivatization reagents are used in LC-MS analysis, part of the method development includes the study of the fragmentation patterns of the derivatives, to choose the transitions that provide the most intense signals which is translated into reaching the highest sensitivity.

Fragmentation of DEEMM derivatives

DEEMM has been used to derivatized amines [59] and amino acids [60], [61] in the past, in case of LC-MS, its derivatives have been studied mainly in positive mode and their fragmentation patterns are well defined. The fragmentation involves the loss of a molecule of ethanol (EtOH) from the precursor ion formed by protonation, $[M+H]^+ \rightarrow [M+H-46]^+$, even though a second molecule of ethanol could be released, when product ion scan was performed over individual amino acid derivatives, product ions in the form $[M+H-92]^+$ were not observed (Figure 11).

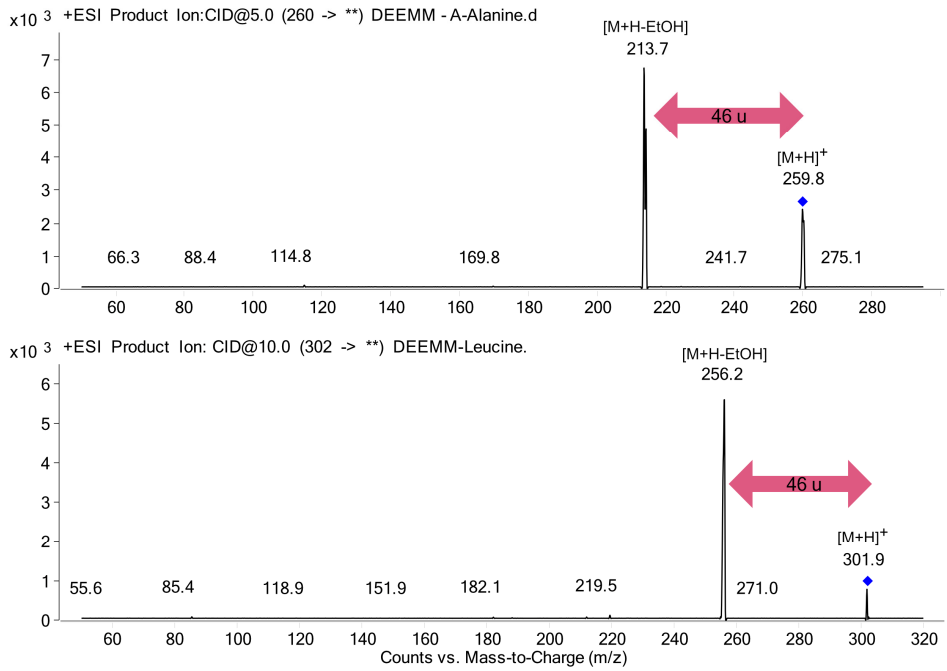

Figure 11. Product Ion Scan mass spectra for DEEMM derivatives of Alanine (top) and Leucine (bottom), only the transition $[M+H]^+ \rightarrow [M+H-46]^+$ is observed at low collision energy voltages in both cases.

Previous studies [58], [61] with negative ionization mode of DEEMM derivatives of amino acids have proposed two main transitions, the first one is the decarboxylation of the deprotonated derivative $[M-H]^- \rightarrow [M-H-44]^-$ and the subsequent loss of ethanol (46 u) to form the ion $[M-H-90]^-$. However, when product ion scans were carried out with individual derivatives, it was discovered that the most intense transitions are actually determined by the structure of the amino acid. For His, Gly, Glu, Pro and Trp derivatives, the extra loss of 46 u (EtOH) was observed, causing product ions of $[M-H-90]^-$. Serine and threonine derivatives, after decarboxylation, lost a water molecule to form the product ions $[M-H-62]^-$ (Figure 12, top for serine). Arg and GABA derivatives had an extra loss of 42 u to create a product ion of $[M-H-86]^-$ (Figure 12, bottom for GABA). Finally, for β-Ala derivative product ion was $[M-H-72]^-$. Therefore, in case of negative ionization mode of DEEMM derivatives of amino acids, a more complex fragmentation process is involved.

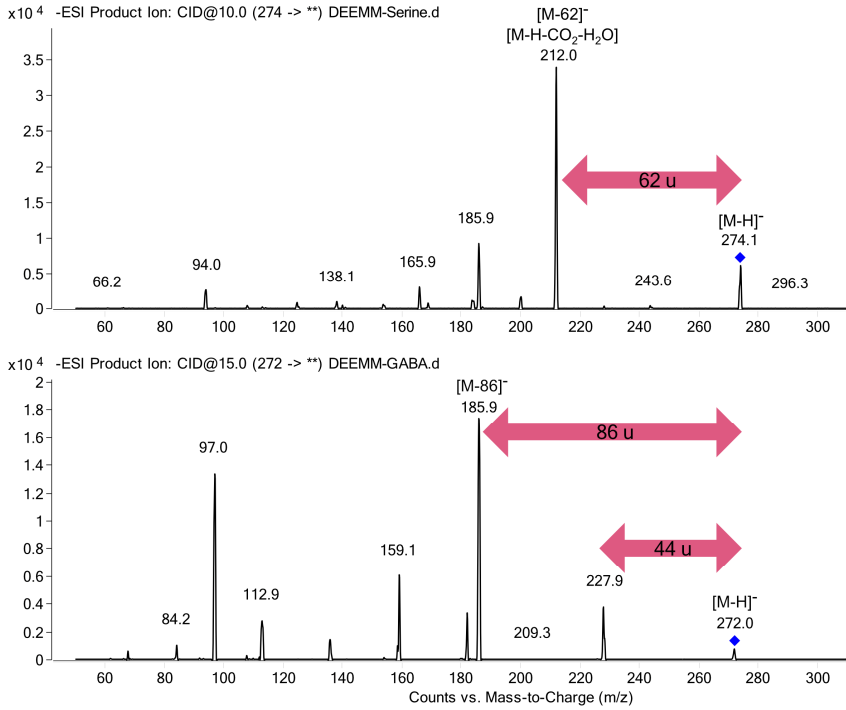

Figure 12. Product ion scan mass spectra of DEEMM derivatives of serine (top) and GABA (bottom) recorded in negative ion mode.

As expected, the loss of two molecules of ethanol from the decarboxylated ion, was not visible in product ion scan studies. Figure 13 illustrates the transitions and the fragmentation sites for DEEMM amino acid derivatives.

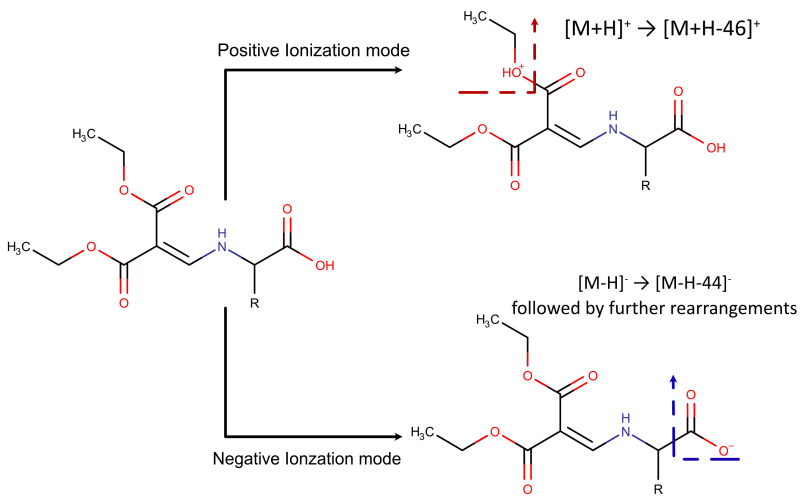

Figure 13. Main fragmentation patterns for DEEMM amino acid derivatives.

AzoB derivatives are disubstituted ureas, and their main fragmentation in positive ion mode is $[M+H]^+ \rightarrow 224$ m/z $(C_6H_5\text{-}N{=}N\text{-}C_6H_4\text{-}NHCO)^+$ with loss of neutral AA that corresponds to the rupture of the ureido bond, this path has been observed in derivatization reagents that also produce disubstituted ureas such as AQC [27], [62], [63] and TAHS [37], [38]. Even though Arg and Trp derivatives also present the main pattern, the transitions $[M+H]^+ \rightarrow 201$ m/z $(C_7H_{13}N_4O_3)^+$ and $[M+H]^+ \rightarrow 188$ m/z $(C_{11}H_{10}NO_2)^+$ respectively, produced more intense peaks.

Besides the previously listed transitions, other fragmentation patterns such as $[M+H]^+ \rightarrow [AA+H]^+$ and $[M+H]^+ \rightarrow 198$ m/z $(C_6H_5\text{-}N{=}N\text{-}C_6H_4\text{-}NH_3)^+$ were identified in product ion scan of amino acid derivatives, but those are not common for all amino acid derivatives, for example it is almost absent in product ion scan of proline and hydroxyproline derivatives (Figure 14). In the case of lysine and ornithine, AzoB is able to react with both amino groups to produce disubstituted derivatives.

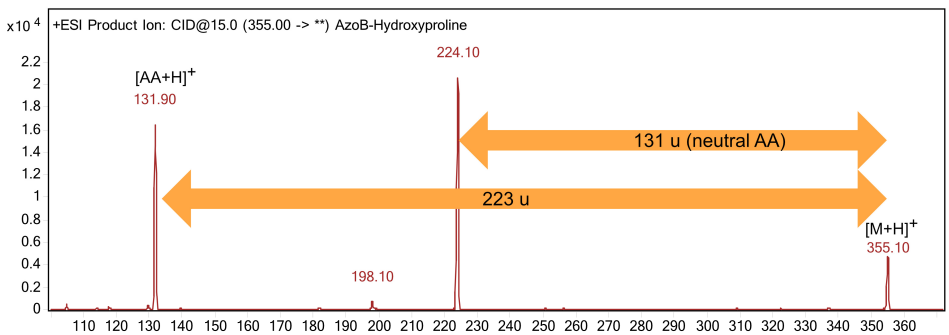

Figure 14. Positive ESI mode product ion scan mass spectrum of AzoB hydroxyproline derivative, fragment ion 198 m/z is very weak compared to all other fragments.

Figure 15 summarizes the way AzoB derivatives fragment when the analysis is performed in positive ionization mode.

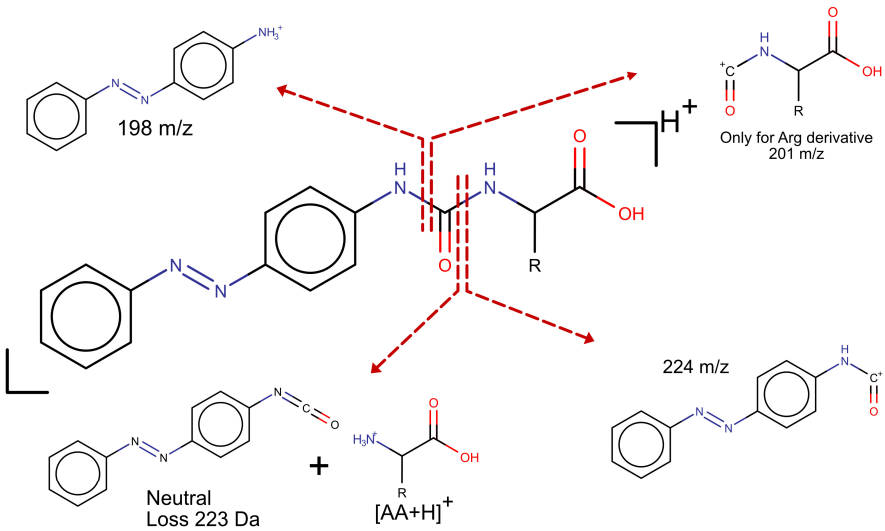

Figure 15. Different fragments observed in AzoB amino acid derivatives when analysis is carried out in positive mode.

In negative electrospray ionization mode, AzoB amino acid derivatives did not show a decarboxylation step as seen with DEEMM derivatives. The dominant fragmentation goes via neutral loss of C_6H_5-N=N-C_6H_4-NCO (223 u) to produce deprotonated amino acids: $[M\text{-}H]^- \rightarrow [AA\text{-}H]^-$ in most of the cases.

Amino acid derivatives of Gly, Leu, Met, Orn, Phe, β-Ala, Val, Tyr, Trp; additionally showed the transition $[M\text{-}H]^- \rightarrow [AA+26]^-$ (where 26 corresponds to conversion of amino group to isocyanate). For the previously mentioned amino acids, this latter transition produced weaker signals, except with glycine derivative, therefore it was used for glycine quantification.

Figure 16 shows the two main transitions for AzoB derivatives in negative mode, contrary to the positive mode, the fragmentation of deprotonated derivatives does not produce a big variety of product ions.

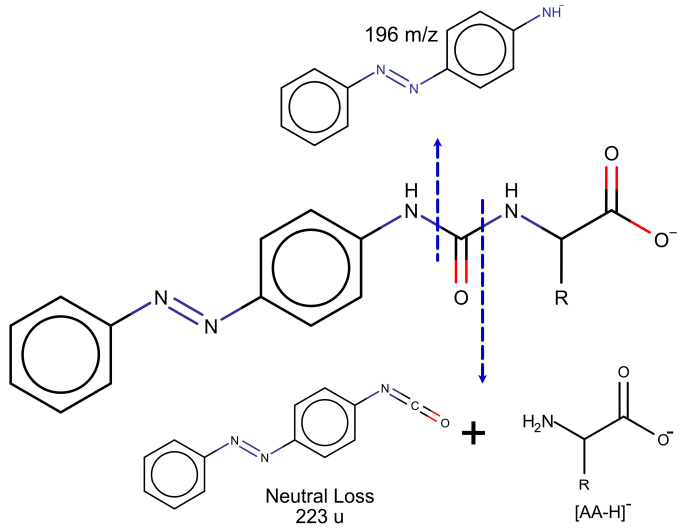

Figure 16. Fragmentation of AzoB amino acid derivatives in negative ionization mode.

It is important to highlight that, when amino acid derivatives were studied with product ion scan mode, the same neutral loss (223 u) was identified in both polarities. To evaluate the repeatability of this behavior, a group of non-proteinogenic amino acids (L-Citrulline, L-Theanine, 5-aminovaleric acid, 2-aminobutyric acid, and 3-aminobutyric acid) was derivatized with AzoB and product ion scan was performed over the respective derivatives. Figure 17 presents the product ion mass spectra for 5-aminovaleric acid (5-AVA) derivative in both polarities. In positive mode, besides protonated derivative (341 m/z), the fragments 224 m/z, 198 m/z, 118 m/z $[5\text{-AVA+H}]^+$ and 100 m/z $[5\text{-AVA-NH}_3]^+$ are present, while in negative mode, alongside deprotonated derivative (339 m/z), fragments 196 m/z, and 116 m/z $[5\text{-AVA-H}]^-$ appeared.

All the non-proteinogenic amino acids derivatives behave the same way as the derivatives of proteinogenic amino acids when product ion scan was performed. Therefore, Neutral Loss Scan (NLS) set to 223 u in both ionization modes can be used to find and confirm the presence of amino acids (both, proteinogenic and non-proteinogenic).

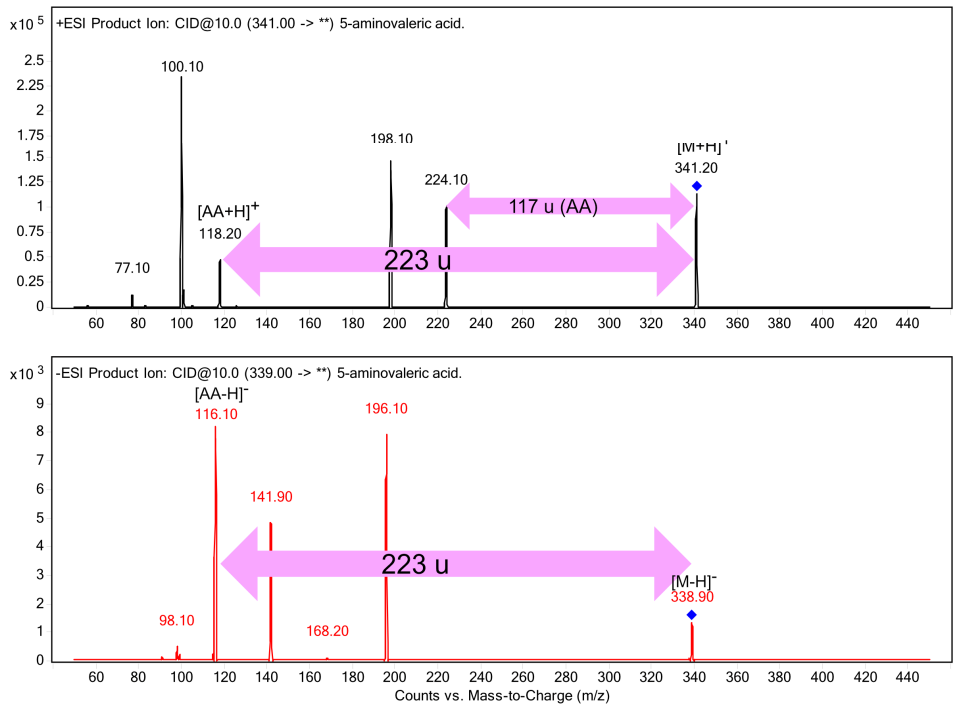

Figure 17. Product ion scan mass spectra for AzoB-5-AVA (5-aminovaleric acid), in positive (top) and negative (bottom), in both cases the loss of 223 Da is visible.

To illustrate the usefulness of AzoB, diluted watermelon juice was derivatized and analyzed by NLS (set to 223 u) in both polarities, alongside studied amino acids group, citrulline was also identified (Figure 18).

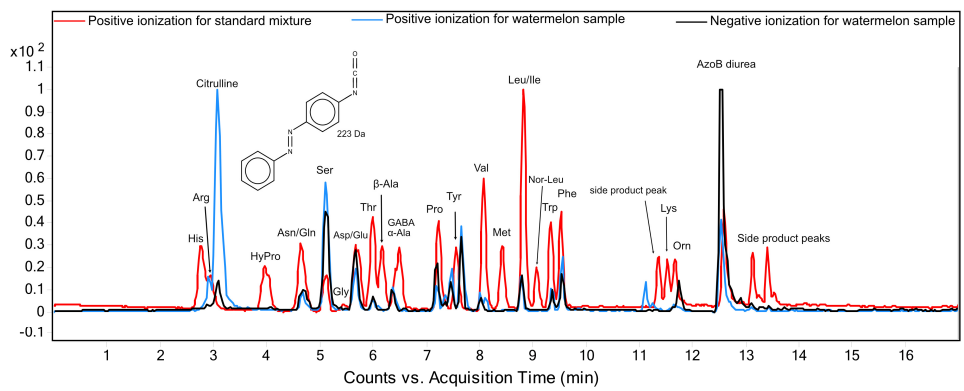

Figure 18. Neutral Loss Scan chromatogram of derivatized watermelon juice, besides the main amino acids analyzed, citrulline, was also identified with NLS in both polarities.

To study the applicability of AzoB to compounds other than amino acids, a group of biogenic amines (BA's) that included tyramine, tryptamine, histamine, phenylethylamine, dopamine, spermidine, agmatine and serotonin was derivatized and analyzed. Despite of forming disubstituted ureas like amino acid derivatives, the product ion scan of biogenic amines derivatives showed that for monosubstituted derivatives their main fragmentation in positive mode was $[M+H]^+ \rightarrow 198$ m/z $(C_6H_5\text{-}N{=}N\text{-}C_6H_4\text{-}NH_3)^+$ instead of 224 m/z, and $[M\text{-}H]^- \rightarrow 196$ m/z $(C_6H_5\text{-}N{=}N\text{-}C_6H_4\text{-}NH)^-$ in negative mode. The difference between precursor and product ion corresponded to the amine Molecular Mass + 26, e.g. in Figure 19, for phenethyl amine derivative (344 g mol^{-1}), the calculated difference is 147 (121, molecular mass of phenethylamine +26).

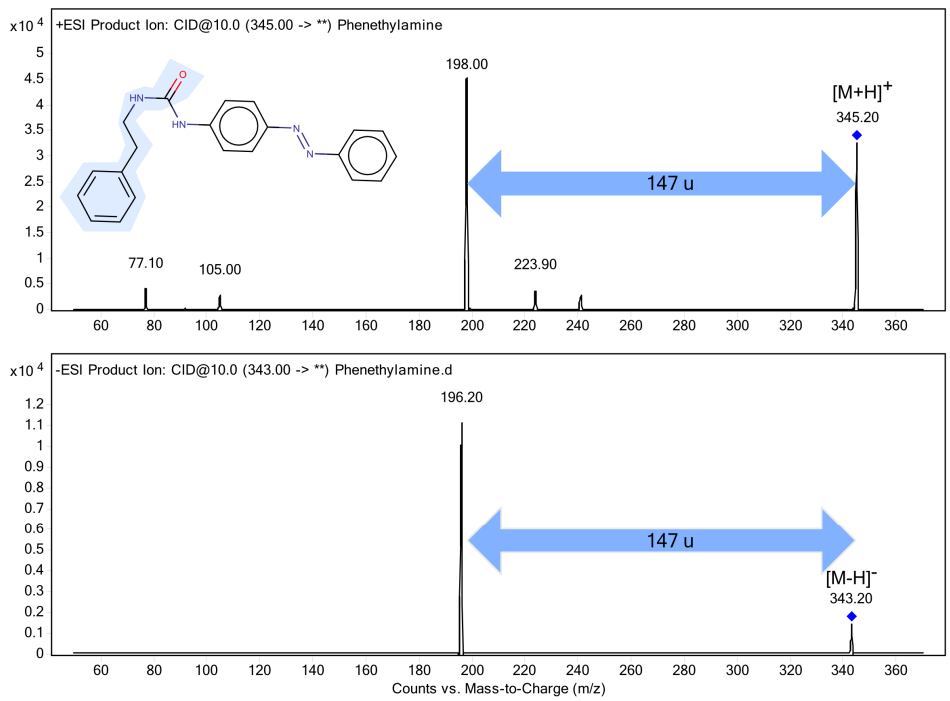

Figure 19. Product ion scan mass spectra of AzoB derivative of phenethyl amine in both ionization modes, the same difference between parent and daughter ions is 147 u.

While for disubstituted derivatives, besides the fragment 196 m/z, the main transition involved the loss of 197 Da $(C_6H_5\text{-}N{=}N\text{-}C_6H_4\text{-}NH_2)$ as it can be seen in Figure 20 for spermidine derivative.

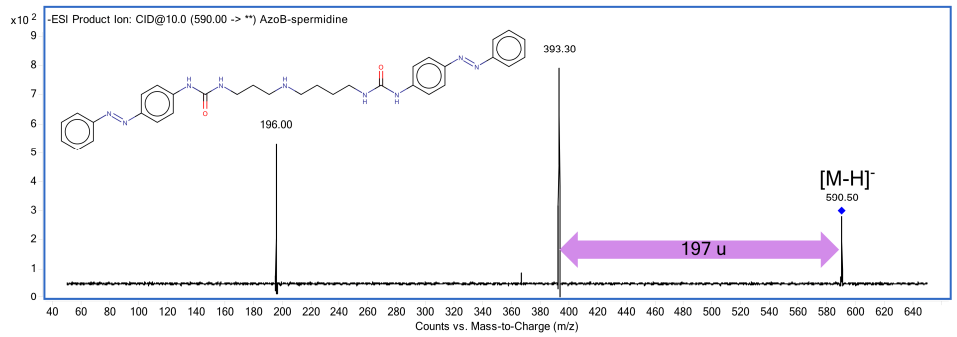

Figure 20. Product ion scan mass spectra for spermidine (diamine) derivative recorded in negative mode.

Because of this not uniform comportment, NLS analysis of amines derivatized with AzoB is less convenient and non-targeted analysis practically impossible. As an alternative, precursor ion scan can be performed since all biogenic amines (even disubstituted ones) produce the fragment ion 198 m/z (+ESI) or 196 m/z (-ESI). Therefore, AzoB provides several options to allow the identification of amino compounds in non-targeted analysis either by Neutral Loss Scan or by Precursor Ion Scan. It also makes possible the differentiation between amines with and without carboxylic acid groups, contrary to AQC where all amino compounds produce the same fragment, [171 m/z] when analyzed in positive ESI [27], [64].

Fragmentation of AzoC derivatives

Differently from AzoB derivatives, AzoC derivatives are amides. In positive mode, all studied derivatives (AA's and BA's) followed the transition $[M+H]^+ \rightarrow$ 209 m/z $(C_6H_5\text{-}N{=}N\text{-}C_6H_4\text{-}C{=}O)^+$ +AA (or BA). Figure 21 shows the mass spectra for a biogenic amine (tyramine, $TyrNH_2$, top) as well as an amino acid (proline, bottom) recorded in positive mode.

On the contrary, fragmentation in negative ionization mode, showed a much more complex behavior, similar to the one observed for DEEMM derivatives in the same polarity. For the amino acid derivatives of His, Gln, Lys, and Orn, the dominant fragmentation was the decarboxylation of the deprotonated derivative $[M\text{-}H]^- \rightarrow [M\text{-}H\text{-}CO_2]^-$ (M-H-44), while for the rest, after the loss of CO_2, several rearrangements were identified, for example, Pro (Figure 22), HyPro, Asp, Gly, Ala and Met, had the transition $[M\text{-}H]^- \rightarrow [M\text{-}H\text{-}72]^-$ (M-H-CO_2-28); or Ser and Thr whose fragmentation pattern was $[M\text{-}H]^- \rightarrow [M\text{-}H\text{-}62]^-$ (M-H-CO_2-H_2O), etc.

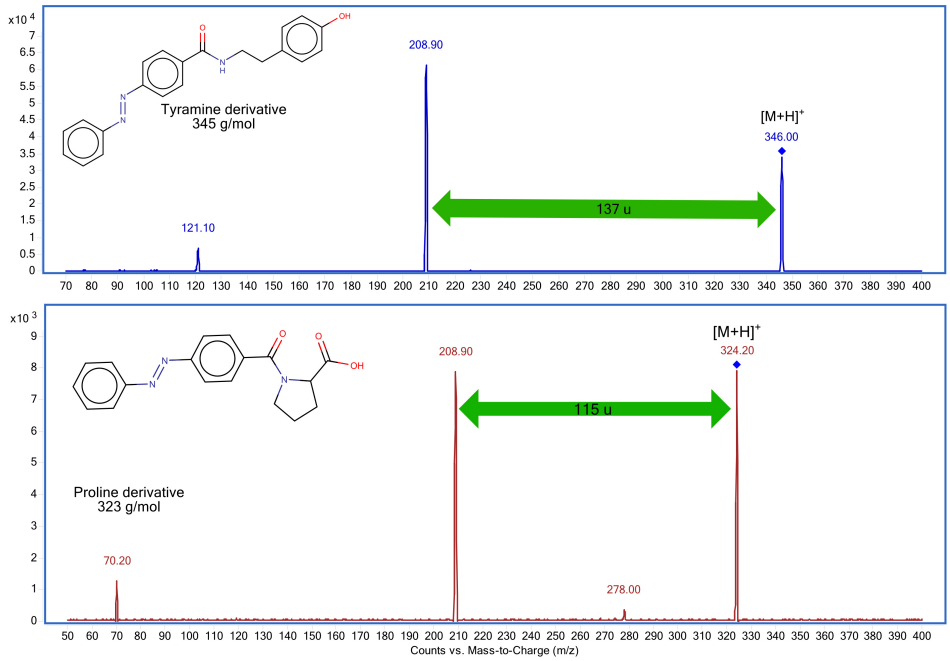

Figure 21. Product ion scan mass spectra of AzoC-TyrNH_2 derivative (top) and AzoC-Pro (bottom), in positive ion mode.

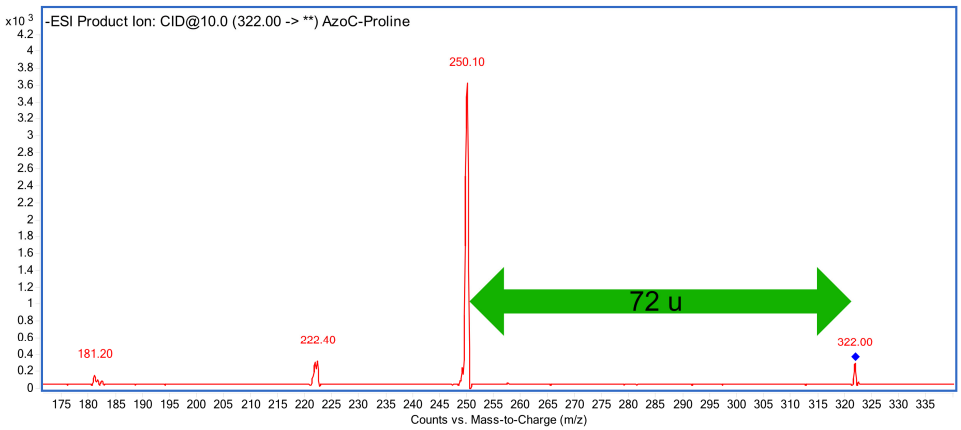

Figure 22. Product ion scan mass spectrum of AzoC derivative of proline in negative ion mode, unlike AzoB, AzoC derivatives have a more complicated fragmentation pattern.

4.1.4 Side reactions affecting derivatization ability

Because of basic media used during the derivatization process, several side reactions affecting the derivatization capability of AzoB and AzoC were identified. First, the alkaline hydrolysis of the succinimide ring (Figure 23 for AzoB), producing an hydroxamate ester that is an isomer of AzoB (or AzoC) aspartic acid derivative. This side reaction has been reported before for succinimidyl carbonates [65]–[67], succinimide as well as other cyclic imides [68] under alkaline conditions.

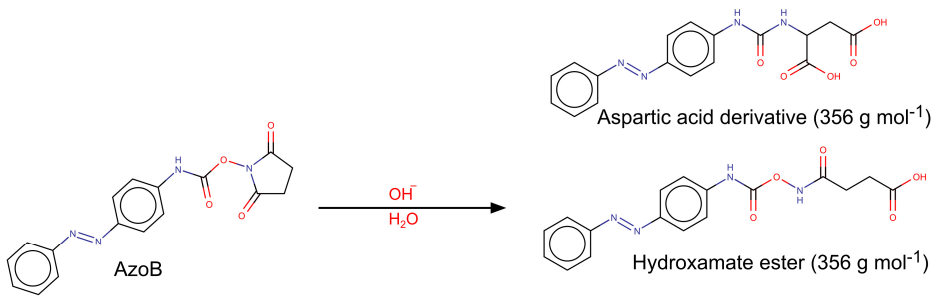

Figure 23. Alkaline hydrolysis over succinimide ring of AzoB. The aspartic acid derivative is shown to make easier the comparison with the hydroxamate ester (hydrolysis product).

In case of AzoB, the hydroxamate ester, elutes next to aspartic acid derivative, which could interfere when determining this amino acid in positive mode, as it also follows the transition 357m/z → 224 m/z. However, if negative ionization mode is used, the observed transition is 355 m/z → 132 m/z is unique for the aspartic acid derivative (Figure 24).

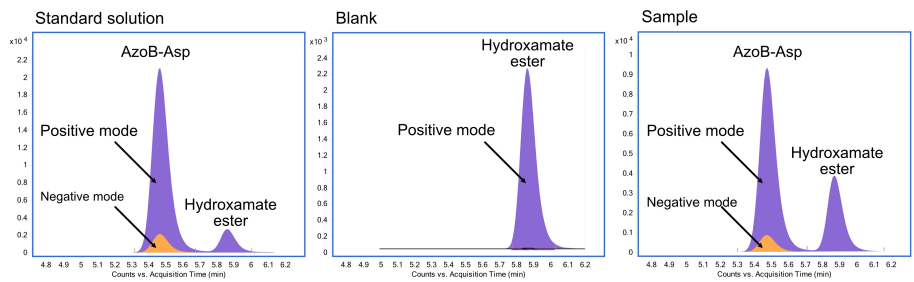

Figure 24. Comparison of chromatograms for AzoB-Asp in standard solution (left), blank (center) and sample (right); when positive mode is used (purple) hydroxamate ester is visible in all cases, contrary to negative ion mode (orange) that only shows aspartic acid derivative in standard and sample solutions.

While for AzoC, both peaks (aspartic and hydroxamate ester) are separated enough to avoid any interference, another problem arose, under the alkaline conditions used for the derivatization, the hydroxamate ester undergoes a Lossen rearrangement that generates free β-alanine which reacts with AzoC to produce its derivative in high yield, mechanism of this reaction is presented in Figure 25.

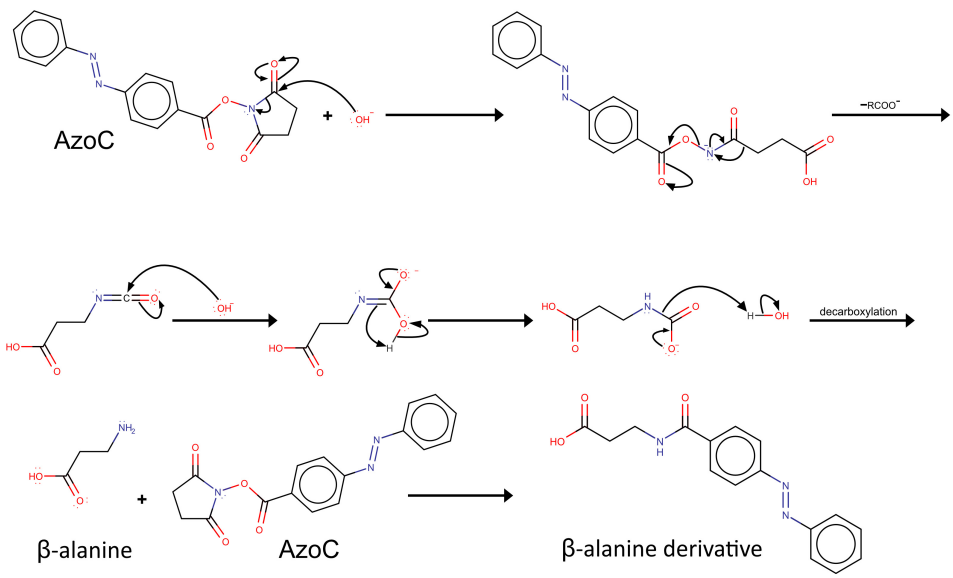

Figure 25. Mechanism of the alkaline hydrolysis of AzoC that leads to the production of free β-alanine which reacts with a second molecule of AzoC generating β-alanine derivative.

The production β-alanine from the hydrolysis of the N-hydroxysuccinimide ring in alkaline media has been reported for other reagents, such as FMOC-Osu (9-Fluorenylmethyl-succinimidyl carbonate) in peptide synthesis [67] where not only β-alanine is produced but also a series of byproducts related to this amino acid.

Since the AzoC derivatives of both β- and α-alanine elute one after the other, the excess of β-alanine derivative strongly affects the quantification of α-alanine in positive mode. Figure 26 shows the peak of AzoC-β-Ala (in orange) that appears both in the blank as well as in a standard solution of α-alanine. In positive ionization mode, peak size of AzoC-α-Ala (in pink) is very small compared to the peak of AzoC-β-Ala. In negative mode, this problem can be avoided because of the used transitions, however, β-alanine cannot be quantified using AzoC.

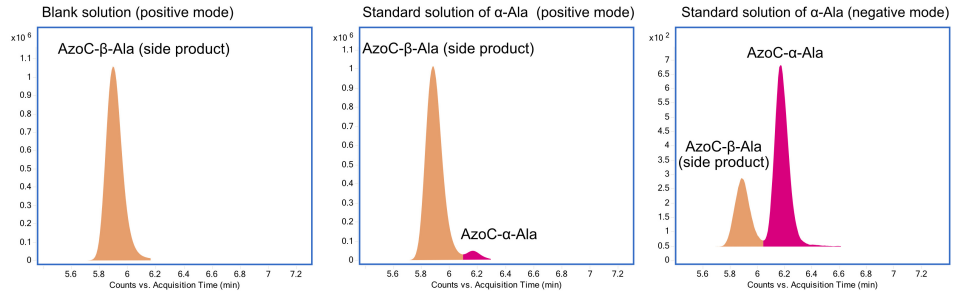

Figure 26. Chromatogram of AzoC solutions: blank in positive mode (left) standard solution only containing α-alanine in positive mode (center) and negative mode (right).

Succinimide ring in AzoC was not only the target of hydrolysis but also alcoholysis reaction (Figure 27), as it has been reported for other compounds containing succinimide in their structures [69], [70].

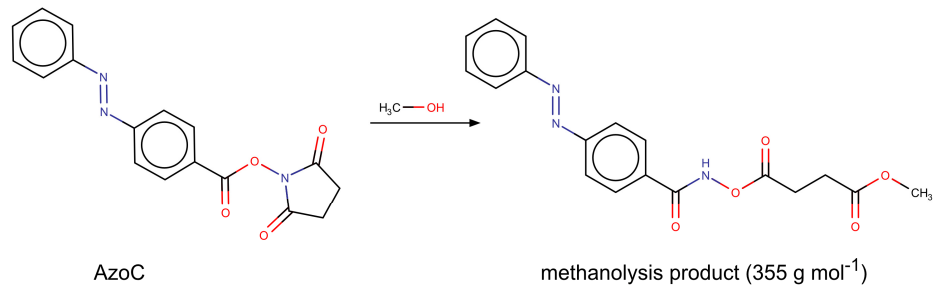

Figure 27. Methanolysis of AzoC.

At early stages of the study with these derivatization reagents, samples and standard solutions were diluted in the same way as stated in paper I (using in 0.1 mol L^{-1} HCl containing 30% MeOH), but it was later discovered the presence of a very intense peak that seemed to be glutamic acid derivative (because of its identical retention time and fragmentation in positive mode) in all derivatized solutions including the blank, this peak was confirmed to be the methanolysis product since it disappeared when MeOH was removed from the solvent used in sample preparation step (Figure 28). AzoB did not show this phenomenon.

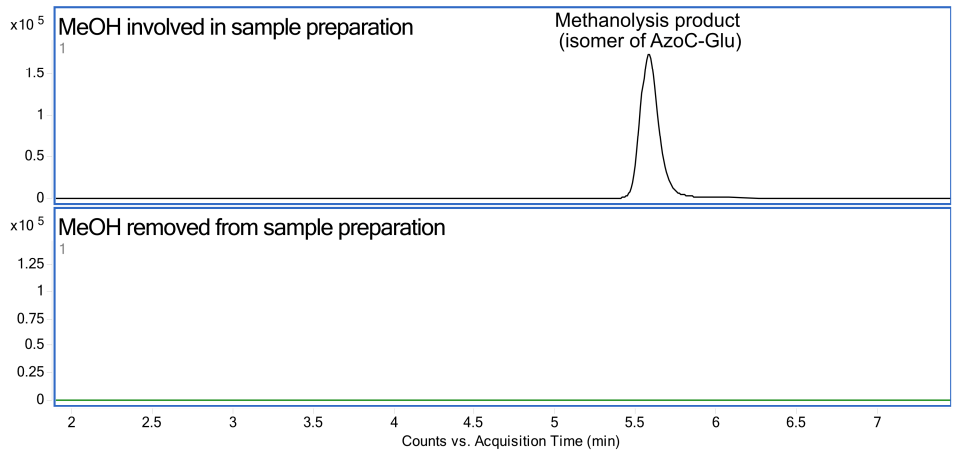

Figure 28. Chromatogram of blank solution derivatized with AzoC before and after removing MeOH from sample preparation step.

4.1.5 Stability of the derivatives

Another important factor to be evaluated is the stability of the derivatives, in case of DEEMM, previous studies have showed that its derivatives are stable after 24 h but must be analyzed before 48 h to obtain reliable results [29]. In case of AzoB, this parameter was tested by derivatizing a solution having all analyzed amino acids, and injecting it into the UPLC system, this vial was kept at room temperature, after 24 h it was re-injected. Amino acid derivatives signals were affected differently. For example, Arg signal was close to constant (decreased less than 5%) while the signal of disubstituted amino acid derivatives (Lys and Orn) decreased by around 20% with respect to their original values. The signals of His, Gln, Asn, Ser, Gly, Asp, Thr, α-ala, GABA, Tyr, Met, and Trp derivatives reduced between 5% and 10%. The rest of the amino acid derivatives signals decreased from 10% to 14%.

4.2 Method Validation (Papers I and II)

To confirm the fitness for purpose of an analytical method, several characteristics such as repeatability, reproducibility, linearity, limits of detection (LoD), limits of quantification (LoQ), etc., must be evaluated.

4.2.1 Repeatability

Repeatability of the system was evaluated by injecting six consecutive times a solution containing all derivatized analytes at two concentration levels. At the lowest level, the relative standard deviation (RSD) was lower than 16% (n = 6

for each derivatization reagent), while at highest level, RSD ranged from 0.8 to 8% (n = 6 for each derivatization reagent), and sample preparation repeatability was between 0.4 and 9%.

4.2.2 Linearity

Linearity and linear range were estimated for each derivatization reagent, for DEEMM the linear range was from 1 to 130 parts per billion (ppb) for each derivative having r^2 values > 0.99, while for AzoB and AzoC methods were linear in the range 6.7 – 1333 nmol L^{-1}, r^2 > 0.993 for AzoB derivatives and r^2 > 0.984 for AzoC derivatives, exceptions were AzoC-α-Ala in positive mode and AzoC-Tyr in negative mode, because those derivatives were affected by side reactions or did not provided a stable signal.

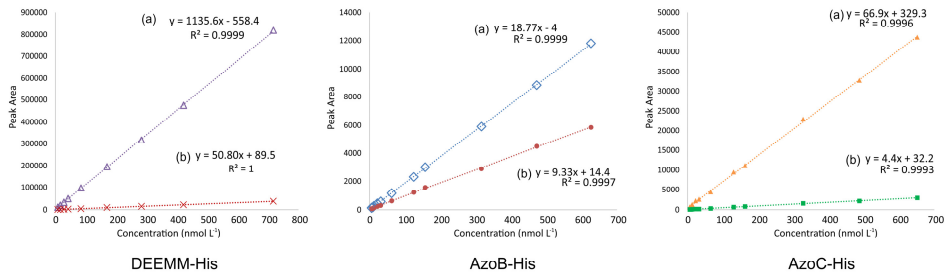

Figure 29. Calibration curves of histidine DEEMM (left), AzoB (center) and AzoC (right) derivatives in positive (a) and negative (b) ionization mode.

In Figure 29, the calibration curves of histidine derivative for the studied derivatization reagents are shown in both polarities, to make their evaluation easier (DEEMM derivative concentration was converted from ppb to nanomolar). Since calibration curves for DEEMM derivatives were recorded on a different instrument, DEEMM, AzoB and AzoC slopes cannot be directly compared, but the general trend is recognizable, slopes in positive (a) mode are higher than in negative (b) mode.

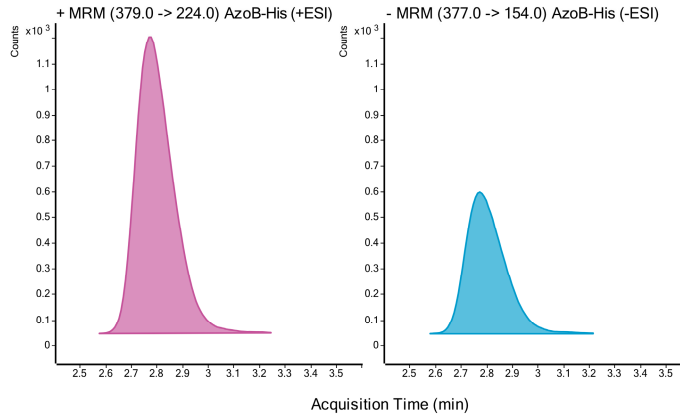

Figure 30. Comparison of peak intensity of AzoB-histidine in positive (left) and negative (right) ionization mode obtained from the analysis of the same solution.

It is well known that positive ionization mode produces more intense signals that negative mode, for example, when analyzing AzoB-His in both ionization modes, the peak size in positive mode is almost twice than in negative mode (Figure 30), however, the results obtained when -ESI was used, are comparable to their counterparts in positive mode.

4.2.3 Estimation of LoD and LoQ

Limits of detection (LoD) and limits of quantification (LoQ) were estimated using equation 1 and equation 2 for each amino acid derivative from the parameters of their respective calibration curves (standard deviation of the residuals, $\sigma_{y/x}$; and slope, S) the estimation was performed for the calibration curves recorded in both ionization modes:

$$LoD = \frac{3\times \sigma_{y/x}}{S} \quad \text{Eq.1}$$

$$LoQ = \frac{10\times \sigma_{y/x}}{S} \quad \text{Eq.2}$$

LoD values, taking into consideration both polarities, ranged (in fmol on column) from 4.1 to 29.7 for DEEMM, for AzoB, from 3.2 up to 58.3 and, finally for AzoC, between 5.9 and 53.3.

From table 5, LoQ values obtained in negative mode, are almost always comparable to their counterparts in positive mode, even though the chosen eluents favor formation of positively charged ions. In positive ionization mode, AzoB offered the lowest LoQ values for 12 amino acids, compared to 8 and 3, from DEEMM and AzoC respectively, while in negative mode, the order is switched, 13 amino acids had the lowest LoQ when DEEMM was used, in the second place, was AzoB with 9 and finally AzoC that only provided the best LoQ for GABA.

Table 5. LoQ values (fmol on column) of amino acid derivatives of the studied derivatization reagents in both positive and negative ion mode.

Amino acid derivative	AzoB		AzoC		DEEMM	
	Pos	Neg	Pos	Neg	Pos	Neg
His	36	46	41	91	16	19
Arg	16	31	46	41	14	22
HyPro	16	22	33	68	--[a]	
Asn	31	28	26	71	31	31
Gln	22	38	23	114	38	42
Ser	149	194	178	177	98	99
Gly	94	171	131	125	58	53
Asp	23	45	58	78	43	63
Glu	19	38	45	76	54	62
Thr	26	62	42	120	70	38
β-Ala	57	132	--[b]		99	41
α-ala	43	65	--[c]	106	69	51
GABA	30	147	46	59	32	63
Pro	40	28	71	83	33	48
Tyr	13	25	20	--[d]	22	26
Val	25	43	49	53	48	31
Met	29	21	58	59	30	16
Leu	58	43	54	66	40	41
Ile	--[e]		29	42	37	36
Trp	15	11	41	29	14	14
Phe	11	16	26	47	16	15
Orn	45	74	48	57	38	31
Lys	48	26	29	34	32	33

[a]Not included in the analysis

[b]Peak affected by side products

[c]Not possible to be estimated in positive mode

[d]Not possible to be estimated in negative mode

[e]Leucine and isoleucine were determined together.

4.2.4 Accuracy and recovery

Accuracy was evaluated by recovery (paper I and II) and by using a certified reference material (CRM) of amino acids (paper II). For DEEMM derivatives, recovery ranged from 93 to 112% throughout three different spiked concentration levels, while for AzoB derivatives recovery ranged between 93% and 108% (RSD < 9%, $n = 6$) and for AzoC from 92% up to 118% (RSD < 12%, $n = 6$).

The accuracy obtained by the analysis of CRM ranged from 91% to 104%, (RSD < 6%, $n = 6$) in case of AzoB derivatives and 92% to 106%, (RSD < 7%, $n = 3$) for AzoC derivatives. In general, it is possible to say that all methods were accurate.

4.2.5 Evaluation of Matrix effect (Paper I)

To evaluate the impact of ME in the determination of amino acids in the analyzed beers, the slopes obtained with standard addition for four samples were compared against the calibration curve acquired with external calibration using equation 3.

$$\%ME = \frac{Slope_{Std.Add}}{Slope_{Ext.Cal.}} \times 100\% \qquad \text{Eq. 3}$$

If the ratio of slopes is 100% it can be stated that there is no matrix effect, for values smaller than 100% signal suppression is observed and for values higher than 100% signal has been enhanced, however, when the ratios are very close to 100% it is almost impossible to define what is the effect impacting the signal.

For practical purposes, the effect is classified as suppression if the ratio of slopes is smaller than 95%, while if %ME is bigger than 105% it is considered as enhancement.

In positive mode, both phenomena (signal suppression and enhancement) were observed, the ratios for suppression ranged from 6 to 23% while ratios for enhancement from 6 up to 24%. In negative mode, on the contrary, signal suppression was vaguely seen in the analyzed samples. However, signal enhancement was the main matrix effect observed, the ratios had an average increase of 7%. Only one atypical value was observed in one sample (39% of enhancement for glutamic acid). As reported before, it is well known that positive ionization mode can be strongly affected by ME, while the negative ionization mode has shown to be less affected by ME [71].

Ratios of slopes for analyzed amino acids in beers are displayed in table 6, for signal suppression, cells are colored in red, while for signal enhancement green color is used.

Table 6. Ratio of slopes obtained with standard addition against external calibration for selected beer samples.

Amino acid	Ratio of slopes in positive mode				Ratio of slopes in negative mode			
	S7	S10	S13	S14	S7	S10	S13	S14
HIS	104%	111%	107%	102%	103%	106%	107%	100%
ARG	104%	106%	105%	106%	91%	99%	102%	104%
ASN	95%	96%	103%	98%	100%	103%	102%	101%
GLN	94%	101%	101%	99%	108%	103%	100%	102%
SER	94%	98%	105%	98%	107%	100%	102%	100%
ASP	90%	100%	102%	102%	106%	93%	102%	103%
GLY	85%	103%	98%	104%	104%	98%	102%	101%
GLU	109%	100%	103%	103%	139%	101%	105%	101%
THR	98%	104%	99%	105%	103%	104%	103%	102%
β-ALA	95%	99%	101%	77%	105%	103%	102%	102%
GABA	80%	94%	102%	97%	105%	104%	99%	106%
α-ALA	88%	100%	100%	103%	108%	107%	102%	104%
Pro	101%	99%	105%	96%	109%	101%	95%	98%
TYR	82%	101%	97%	100%	100%	102%	103%	102%
MET	107%	104%	103%	109%	103%	98%	102%	103%
VAL	93%	100%	103%	99%	104%	104%	106%	102%
TRP	85%	98%	103%	99%	106%	100%	105%	101%
ORN	92%	96%	100%	103%	101%	99%	103%	101%
PHE	84%	100%	98%	101%	106%	101%	102%	101%
ILE	103%	105%	109%	101%	97%	99%	107%	103%
LEU	96%	94%	112%	101%	106%	104%	104%	103%
LYS	124%	116%	121%	105%	104%	101%	100%	102%

4.3 Ionization efficiency (Paper II)

One important parameter to be evaluated, when new derivatization reagents are being studied, is their ionization efficiency (IEff), for this purpose, AzoB and AzoC derivatives of Gly, Pro and Phe were synthesized in-house, those amino acids were chosen because they encompass primary amines (Gly and Phe), secondary amines (Pro), and hydrophobic aromatic (Phe).

Since absolute ionization efficiency is affected by several factors such as ion source geometry, its cleanliness as well as eluent composition, it is difficult to measure absolute IEff directly. One way to overcome this problem is to measure the relative ionization efficiency (RIE), which is the ratio of absolute IEff values of the compounds, where the IEff value of the compound of interest (M_1)

is measured against a reference compound (M_2) by dividing the slopes [72] of their calibration curves according to equation 4.

$$RIE\left({}^{M_1}/_{M_2}\right) = \frac{slope(M_1)}{slope(M_2)} \quad \text{Eq. 4}$$

To simplify the evaluation of the RIE of the different derivatives, logarithmic scale is used (log*IE*) as it allows to compare the obtained values with the data from our research group [72].

Single solutions of the different pure derivatives of AzoB and AzoC were prepared in a mixture of 0.1% aqueous formic acid and acetonitrile (20:80 v/v) at the same concentration range used in the determination of amino acids in samples. The calibration curves were obtained and compared against FMOC-Phe (log*IE* 2.67) in positive mode.

Table 7. LogIE values as well as LoQ values of the studied compounds.

Compound	log*IE* against FMOC-Phe	$LoQ_{\text{fmol on column}}$ (positive mode)
AzoB-Phe	0.98	11
AzoB-Pro	0.73	40
AzoB-Gly	0.67	94
AzoC-Phe	0.59	26
AzoC-Pro	0.56	71
AzoC-Gly	0.03	131

Table 7 presents the log*IE* values for the different amino acid derivatives. Since IEff has impact on LoD and LoQ values, it is expected that the compound with the lowest LoQ value has a high ionization efficiency, for example AzoB-Phe has the highest log*IE* value, 0.98, and the lowest limit of quantification, 11 fmol on column.

Since one of the goals of derivatization is improve the ionization efficiency of analytes, based on the previously reported data [72], the log*IE* values of the derivatives are higher than the underivatized amino acids as it can be seen from Figure 31.

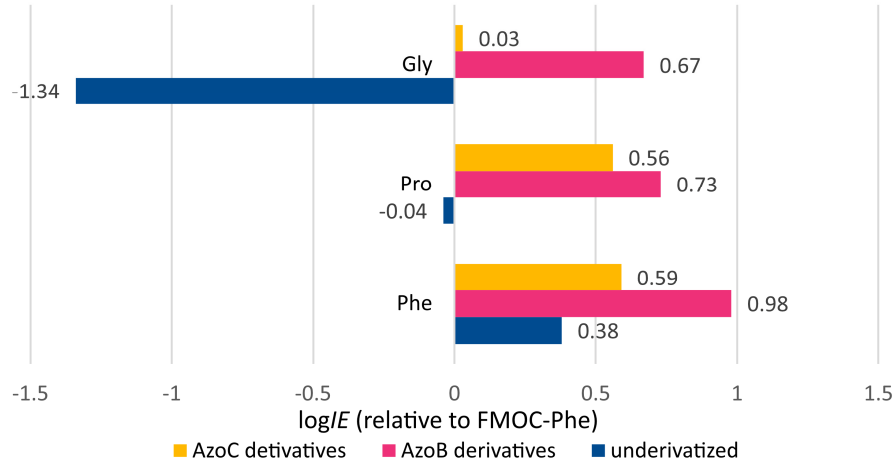

Figure 31. Comparison of logIE of underivatized amino acids and their derivatives.

4.4 Utility of negative ionization mode as identity confirmation tool (Paper III)

Since AzoB derivatives showed a good performance in both ionization modes, the application of negative transitions to provide qualifier ions was explored. Identity confirmation is performed by the comparison of ratios of quantifier/ qualifier from samples against the ones obtained from standard solutions, these ratios are calculated using the equations 5 and 6:

$$Ion\ ratio_{calibration} = \frac{peak\ area\_calibrant_{negative\ mode}}{peak\ area\_calibrant_{positive\ mode}} \quad \text{Eq. 5}$$

$$Ion\ ratio_{sample} = \frac{peak\ area\_sample_{negative\ mode}}{peak\ area\_sample_{positive\ mode}} \quad \text{Eq. 6}$$

To calculate the ion ratios, a set of eleven calibrant solutions as well as the samples were prepared and measured as stated in experimental section. Because of the software used to perform the quantitative analysis did not allow to use qualifier ions from a different polarity, the ion ratios had to be calculated using Microsoft Excel spreadsheet software.

To assess the compliance of the calculated ion ratios with the validation guidelines, equation 7 was used and the results were compared against the limits established by the guidelines. SANTE/11313/2021 determines the tolerance (maximum relative difference) as ± 30%, [56], while guideline 2021/808 sets it to ± 40% [57] irrespective of the qualifier/quantifier ratio (originally in paper III, results were evaluated according to the criteria set by 2002/657/EC, but since this guideline was updated, in this work, results were re-evaluated according to the new legislation).

$$\%\ Relative\ difference = \frac{Ion\ ratio_{sample} - Ion\ ratio_{calibration}}{Ion\ ratio_{calibration}} \times 100 \qquad \text{Eq. 7}$$

The results of the calculations of relative differences of ion ratios for the amino acid derivatives in the samples are presented in table 8. Derivatives can be categorized in 3 groups according to their reference ion ratio (from calibration): amino acid derivatives whose qualifier/quantifier ratios are smaller than 0.1 (Arg, Ser, α-Ala, β-Ala, GABA); derivatives with a reference ion ratio higher than 0.5 (His, HyPro, Asn, Gln, Pro, Orn, Lys) and the major group that contain amino acids derivatives with ratios around 0.2. It must be highlighted that no correlation between the qualifier/quantifier ratio and amino acid content was found. To illustrate this point, in tomato juice, GABA is the second most abundant amino acid (782,6 mg L^{-1}) and the reference value for this derivative is the lowest among all derivatives (0.02) and its relative difference to the reference ion ratio is -5%, while in watermelon juice, GABA's concentration is around 8 times lower (101.9 mg L^{-1}) and the relative difference from the reference ion ratio is 8%.

Table 8. Calculated relative differences of ion ratios for the analyzed samples.

Amino acid derivative	Reference value (*Ion ratio*$_{calibration}$)	Tomato juice		Watermelon juice		Kali		CRM	Relative difference tolerance limit	
		Relative difference	Content (mg L^{-1})	Relative difference	Content (mg L^{-1})	Relative difference	Content (mg L^{-1})	Relative difference	SANTE/11312/2021	2021/808
GABA	0.02	-5%	782.6	8%	101.9	-3%	2	---[x]	± 30 %	± 40 %
β-Ala	0.03	-1%	14.3	-1%	15.1	---[A]		---[x]		
Ser	0.04	-18%	111.4	-7%	43.9	---[B]		-2%		
α-Ala	0.04	-4%	39.7	-4%	90.9	-3%	2.3	-4%		
Arg	0.06	-5%	66.5	-3%	335.33	-13%	1	6%		
Gly	0.17	-26%	11.8	-23%	4.7	---[B]		-27%	± 30 %	± 40 %
Leu-Ile	0.18	-4%	61.8	-5%	52.2	-4%	3.7	-5%		
Phe	0.2	-6%	108.3	-6%	57.9	-6%	1.7	-6%	± 30 %	± 40 %
Asp	0.22	25%	586.2	-5%	169.4	-11%	1.5	-4%		
Glu	0.23	17%	3386.6	-1%	231.1	-6%	1.3	2%		
Val	0.23	9%	12.8	16%	18.8	25%	1.2	-16%		
Met	0.23	-4%	7.1	-3%	4.8	---[B]		-6%		
Thr	0.25	-11%	124.9	-7%	21.8	-13%	0.8	-4%		
Tyr	0.25	-7%	19.7	-9%	5.5	-8%	1.4	-6%		
Trp	0.25	-6%	10.3	-7%	32.4	---[A]		---[x]		
Orn	0.52	---[A]		8%	3.1	---[A]		-3%	± 30 %	± 40 %
Pro	0.56	-7%	34.8	-6%	30.3	-8%	8.4	-0.40%		
His	0.57	-17%	64.4	-14%	27.2	---[B]		-4%		
Lys	0.58	8%	59.4	2%	19.6	---[A]		2%		
Asn	0.63	-13%	305.2	-10%	42.8	-15%	1	---[x]		
HyPro	0.77	---[A]		---[A]		---[A]		---[x]		
Gln	0.84	---[A]		-11%	731.7	---[A]		---[x]		

[A] - Not detected in sample
[B] - Below limit of quantitation
[x] - Amino acids absent in the Certified Reference Material

4.5 Amino acid profiles of analyzed samples

In food and beverages, the presence of free amino acids along other chemical compounds, affects their organoleptic properties such as smell, taste, etc. For example, it has been reported that Gly and L-Ala show sweetness, L-Phe, L-Tyr, L-Val, and L-Ile exhibit a bitter flavor while Glu and Asp are sour, but as sodium salts they produce the umami flavor [73], [74].

4.5.1 Free amino acids in beers (Paper I)

As expected, for fermented beverages, proline was found to be the most abundant amino acid (concentration range: 190 – 1130 ppm), since it is not consumed during the fermentation step [75], [76]. GABA, α-alanine, tyrosine, arginine, and asparagine were found in high concentration, while amino acids such as threonine, methionine, β-alanine, and ornithine were not detected/quantified in most of the samples.

Samples were analyzed on different dates over a period of one year and no decrease in the amino acid content were not found.

Table 9 presents the results of the determination of free amino acid content in both positive and negative ionization mode for the 15 analyzed samples. Values obtained in both polarities are similar to each other.

Table 9. Average content of free amino acids (ppm) in analyzed beers in positive (POS) and negative (NEG) ionization modes.

Amino	S1		S2		S3		S4		S5		S6		S7		S8		S9		S10		S11		S12		S13		S14		S15	
acid	POS	NEG	POS	NEG	POS	NEG	POS	NEG	POS	NEG	POS	NEG	POS	NEG	POS	NEG	POS	NEG	POS	NEG	POS	NEG	POS	NEG	POS	NEG	POS	NEG	POS	NEG
HIS	23.6	23.1	31.6	32.2	20.3	19.3	32.0	30.6	17.4	16.4	3.9	4.0	38.7	36.7	36.7	37.9	18.2	19.0	28.6	31.0	26.1	28.3	52.3	54.9	36.1	38.4	28.5	29.7	33.5	34.3
ARG	41.4	42.2	71.1	74.7	29.7	29.9	57.7	56.6	30.9	31.5	12.5	11.9	56.2	56.3	91.2	91.8	31.6	32.1	140.4	150.0	53.7	57.5	46.5	45.9	100.2	105.4	60.7	63.4	27.1	26.3
ASN	30.6	32.8	18.0	19.8	NQ	NQ	4.5	4.5	3.4	3.2	2.3	2.1	9.7	12.4	244.2	250.7	82.4	87.5	264.9	280.1	91.3	98.2	43.2	47.8	230.9	236.2	16.6	19.6	48.9	53.6
GLN	13.6	14.5	32.7	32.6	4.2	4.3	5.3	5.4	12.4	12.9	3.3	4.1	4.3	4.7	10.9	13.0	9.4	9.0	31.9	30.4	16.1	17.5	23.8	22.9	12.9	11.6	8.9	12.4	25.2	23.5
SER	14.4	17.3	16.0	17.0	NQ	NQ	NQ	NQ	NQ	NQ	4.0	4.8	6.8	7.9	NQ	16.1	21.3	22.1	NQ	NQ	NQ	NQ	30.2	30.0	ND	ND	NQ	NQ	18.6	16.8
ASP	30.4	31.6	52.8	54.4	NQ	NQ	11.4	10.6	3.3	2.6	5.1	5.0	34.9	37.2	27.4	30.0	17.7	17.6	38.0	34.0	27.7	27.3	36.7	34.2	13.2	NQ	26.0	26.0	32.9	30.2
GLY	8.6	11.7	34.1	37.3	15.4	15.2	25.2	27.5	20.9	19.4	6.6	7.4	21.0	26.7	32.6	35.7	NQ	8.1	40.1	45.0	23.9	27.9	72.0	74.9	23.9	26.0	22.8	27.3	32.7	31.6
GLU	48.4	52.6	49.6	59.9	11.4	12.6	38.4	39.7	13.9	15.7	8.3	8.1	65.0	72.7	86.8	85.0	37.8	38.7	71.2	77.4	71.8	75.1	80.2	84.8	39.6	40.3	57.9	62.4	44.9	46.6
THR	ND	ND	10.5	10.2	NQ	ND	ND	NQ	ND	NQ	2.9	3.5	3.9	5.0	NQ	11.0	NQ	8.8	NQ	6.7	ND	NQ	17.6	18.8	NQ	NQ	NQ	8.0	14.7	13.9
β-ALA	NQ	NQ	NQ	NQ	NQ	1.3	NQ	1.6	NQ	1.6	NQ	NQ	NQ	2.0	ND	NQ	ND	NQ	ND	NQ	NQ	NQ	ND	NQ	ND	ND	ND	NQ	ND	NQ
GABA	24.1	25.9	86.2	85.4	50.2	54.2	78.4	76.8	62.2	63.4	7.0	8.3	47.4	49.5	168.0	166.8	154.4	155.4	140.4	147.6	80.4	79.1	241.5	243.0	84.4	82.5	111.8	111.5	66.9	63.0
α-ALA	49.1	47.2	105.1	100.0	47.5	48.7	93.3	92.8	69.0	67.9	9.0	10.1	122.6	121.6	202.5	192.3	196.2	187.2	130.8	125.9	116.3	109.0	333.5	311.0	130.4	120.8	145.0	141.4	57.1	53.3
PRO	305.8	305.8	322.2	319.2	329.5	326.4	480.9	441.2	363.9	364.5	198.5	194.7	595.2	592.1	682.1	726.7	404.0	410.1	568.4	602.2	506.7	529.7	1069.0	1127.3	739.6	760.4	326.6	325.6	383.9	395.1
TYR	37.7	39.0	84.1	84.1	39.5	40.7	73.1	75.9	24.8	24.5	4.7	5.3	72.9	77.2	123.7	122.0	6.4	7.7	117.3	119.6	57.5	61.0	210.2	212.8	92.6	92.3	74.2	76.1	84.0	84.9
MET	4.6	5.0	16.8	15.4	ND	ND	2.0	2.3	ND	NQ	2.7	3.4	8.0	8.7	7.8	6.5	ND	NQ	NQ	NQ	NQ	NQ	17.5	17.0	ND	NQ	8.9	7.2	8.1	8.5
VAL	38.4	40.7	84.4	81.6	27.7	29.6	57.2	57.8	12.8	12.9	8.1	8.3	75.9	78.4	135.7	135.1	NQ	7.0	84.3	85.0	39.2	39.7	209.2	211.4	99.0	96.7	71.8	71.6	49.4	49.6
TRP	18.7	20.2	25.8	28.7	17.2	18.6	26.3	27.7	15.6	15.7	3.6	3.7	22.7	26.3	37.0	39.9	NQ	NQ	39.8	41.1	25.3	26.5	54.7	57.0	45.7	47.0	27.8	30.4	31.1	33.0
ORN	NQ	NQ	2.3	2.6	NQ	1.5	NQ	1.7	1.6	1.9	2.4	2.8	NQ	2.3	9.6	14.5	10.6	11.4	10.7	9.9	ND	ND	71.6	74.6	NQ	NQ	NQ	12.7	9.7	7.9
PHE	41.3	45.4	82.9	83.7	25.0	26.3	52.5	54.8	9.5	9.0	8.5	9.1	79.6	87.9	101.2	105.7	4.5	4.2	91.3	95.6	36.0	38.6	191.8	197.1	83.1	84.4	68.0	73.2	46.1	48.1
ILE	19.1	19.5	39.8	39.9	4.6	4.5	15.4	15.8	ND	NQ	7.6	7.2	36.6	32.9	32.5	28.3	NQ	ND	12.8	12.3	9.4	7.2	58.2	49.2	20.3	17.1	24.1	18.1	14.7	14.4
LEU	36.3	36.7	94.0	95.3	7.9	7.7	29.5	28.0	3.0	2.5	16.9	17.2	82.4	83.9	61.0	63.4	NQ	8.0	48.4	50.4	13.2	14.1	130.3	132.2	38.2	39.5	50.8	52.5	42.6	46.0
LYS	17.4	20.4	17.9	19.8	7.0	7.6	15.9	20.1	ND	NQ	3.4	4.1	21.4	30.0	8.9	13.5	NQ	NQ	10.9	10.6	NQ	NQ	21.1	20.8	NQ	NQ	NQ	8.0	15.2	13.6

ND: not detectable; NQ: not quantifiable.

4.5.2 Free amino acids in kali and juices (Paper II)

Similar to beers, the content of proline in kali was the highest among all amino acids with a concentration ranging from 5 to 9 mg L^{-1}. Arg, Asn, Thr, α-Ala, GABA, Tyr, Val, Leu/Ile, and Phe were present in two of the four analyzed samples. Aspartic acid besides proline, was found in all Kali samples. The content of His, HyPro, Gln, β-Ala, Trp, Orn and Lys was too low to be detectable in the samples.

About the juices, HyPro was not detected in any of them; The content of arginine, glutamine, aspartic, glutamic acid, and GABA was high in watermelon juice. As expected, in tomato juice very high content of glutamic acid was determined. Amino acids such as GABA, Asp, Phe, Ser, Asn and Thr were found in concentrations higher than 100 mg L^{-1}. In general, low concentration of glycine, β-alanine, methionine was found in juices.

Results obtained with AzoB (table 10) agree with the values found with AzoC (table 11), except for AzoC-α-ala since it was not possible to quantify it in positive mode and AzoC-β-ala was not determined because of interference by side products (section 4.1.4).

Table 10. Amino acid profile of analyzed samples with AzoB. Amino acid content is expressed as mg L^{-1}.

	Kali1				Kali2				Kali3				Kali4				Watermelon Juice				Tomato Juice			
Amino acid	Pos	%RSD (n=6)	Neg	%RSD (n=6)	Pos	%RSD (n=6)	Neg	%RSD (n=6)	Pos	%RSD (n=6)	Neg	%RSD (n=6)	Pos	%RSD (n=6)	Neg	%RSD (n=6)	Pos	%RSD (n=12[A])	Neg	%RSD (n=12[B])	Pos	%RSD (n=9[C])	Neg	%RSD (n=9[D])
His	NQ	---	ND	---	ND	---	ND	---	NQ	---	NQ	---	NQ	---	NQ	---	27.5	7%	28.8	7%	64.6	3%	65.5	6%
Arg	NQ	---	NQ	---	ND	---	ND	---	1.0	3%	1.0	8%	1.0	8%	1.0	13%	335.3	2%	328.9	5%	66.5	4%	66.8	4%
HyPro	ND	---	ND	---	ND	---	ND	---	ND	---	ND	---	ND	---	ND	---	ND	---	ND	---	ND	---	ND	---
Asn	0.8	3%	0.8	7%	ND	---	ND	---	1.0	5%	0.9	8%	1.0	8%	1.0	7%	42.8	5%	42.5	4%	305.2	3%	302.8	2%
Gln	ND	---	ND	---	ND	---	ND	---	ND	---	ND	---	ND	---	ND	---	731.7	2%	704.0	4%	ND	---	ND	---
Ser	NQ	---	NQ	---	ND	---	ND	---	NQ	---	NQ	---	NQ	---	NQ	---	43.9	6%	46.5	8%	111.4	5%	98.6	8%
Gly	NQ	---	NQ	---	ND	---	ND	---	NQ	---	NQ	---	NQ	---	NQ	---	4.7	4%	4.9	16%	11.8	2%	12.2	2%
Asp	3.5	4%	3.5	3%	1.3	10%	1.4	7%	1.5	7%	1.5	11%	1.5	3%	1.5	4%	169.4	3%	166.7	5%	586.2	4%	595.1	3%
Glu	NQ	---	NQ	---	NQ	---	NQ	---	1.3	12%	1.4	18%	1.3	2%	1.4	8%	231.1	3%	225.0	5%	3386.6	10%	3022.9	2%
Thr	0.6	8%	NQ	---	ND	---	ND	---	0.8	1%	0.7	6%	0.8	11%	0.7	12%	21.8	4%	20.8	10%	124.9	3%	122.3	3%
β-Ala	ND	---	ND	---	ND	---	ND	---	ND	---	ND	---	ND	---	ND	---	15.1	5%	13.0	24%	14.3	3%	14.4	13%
α-Ala	3.3	2%	3.3	6%	NQ	---	NQ	---	2.3	1%	2.4	0.1	2.3	4%	2.4	4%	90.9	3%	89.8	5%	39.7	7%	42.1	2%
GABA	0.8	5%	NQ	---	ND	---	ND	---	2.0	5%	NQ	---	2.0	2%	1.9	11%	101.9	3%	102.4	5%	782.6	3%	767.8	3%
Pro	5.6	0.5%	6.7	1%	8.2	0.3%	8.4	16%	8.5	2%	9.0	16%	8.4	2%	9.0	8%	30.3	2%	31.6	9%	34.8	7%	37.3	4%
Tyr	1.0	2%	1.0	7%	NQ	---	NQ	---	1.5	3%	1.5	5%	1.4	3%	1.4	8%	5.5	12%	6.2	10%	19.7	4%	21.4	6%
Val	1.5	2%	2.4	3%	NQ	---	NQ	---	1.2	2%	1.8	3%	1.2	2%	1.8	2%	18.8	9%	23.3	3%	12.8	3%	22.5	3%
Met	NQ	---	NQ	---	ND	---	ND	---	NQ	---	NQ	---	NQ	---	NQ	---	4.8	2%	5.3	4%	7.1	1%	7.6	2%
Leu	3.6	3%	3.7	0.0	NQ	---	NQ	---	3.8	0.5%	3.9	3%	3.7	4%	3.8	5%	52.2	3%	52.2	2%	61.8	7%	63.6	5%
Ile	Quantified along with leucine.																							
Trp	ND	---	ND	---	ND	---	ND	---	ND	---	ND	---	ND	---	ND	---	32.4	5%	32.5	3%	10.3	1%	11.4	6%
Phe	1.5	2%	1.5	5%	NQ	---	NQ	---	1.8	1%	1.8	4%	1.7	5%	1.8	6%	57.9	4%	58.0	3%	108.3	3%	108.0	3%
Orn	ND	---	ND	---	ND	---	ND	---	ND	---	ND	---	ND	---	ND	---	3.1	2%	2.5	14%	ND	---	ND	---
Lys	ND	---	ND	---	ND	---	ND	---	ND	---	ND	---	ND	---	ND	---	19.6	6%	19.7	10%	59.4	8%	61.2	4%

[A] For His, Arg, Asn, Asp, Glu, α-Ala, Trp, and Phe, n = 15; Gly, n = 5; Met, n = 6; and Orn n = 3.

[B] For His, Arg, Asn, Asp, Glu, Thr, α-Ala, Trp, and Phe, n = 15; Gly, n = 5; Met, n = 6; and Orn n = 5.

[C] For Asn, GABA, Tyr, n= 6; Gly, β-Ala, Val, Met, Trp n = 3.

[D] For Asn, Ser, Asp, GABA, Pro, Tyr, Val, n= 6; Gly, Glu, β-Ala, Met, n = 3.

ND: not detectable; NQ: Not quantifiable.

Table 11. Amino acid profile of analyzed samples with AzoC. Amino acid content is expressed as mg L^{-1}.

	Kali1				Kali2				Kali3				Kali4				Watermelon Juice				Tomato Juice			
Amino acid	Pos	%RSD (n=3)	Neg	%RSD (n=3)	Pos	%RSD (n=3)	Neg	%RSD (n=3)	Pos	%RSD (n=3)	Neg	%RSD (n=3)	Pos	%RSD (n=3)	Neg	%RSD (n=3)	Pos	%RSD (n=12[E])	Neg	%RSD (n=12[F])	Pos	%RSD (n=9[G])	Neg	%RSD (n=9[H])
His	ND	---	ND	---	ND	---	ND	---	ND	---	ND	---	ND	---	ND	---	28.6	3%	28.0	8%	62.4	8%	64.3	8%
Arg	ND	---	NQ	---	ND	---	NQ	---	0.9	3%	NQ	---	NQ	---	NQ	---	377.2	2%	352.9	5%	72.8	6%	64.8	8%
HyPro	ND	---	ND	---	ND	---	ND	---	ND	---	ND	---	ND	---	ND	---	ND	---	ND	---	ND	---	ND	---
Asn	0.9	3%	0.9	11%	ND	---	ND	---	1.1	6%	1.2	15%	1.1	4%	0.9		48.4	6%	48.3	6%	344.8	2%	341.1	8%
Gln	ND	---	ND	---	ND	---	ND	---	ND	---	ND	---	ND	---	ND	---	724.6	2%	672.1	10%	ND	---	ND	---
Ser	NQ	---	NQ	---	ND	---	ND	---	NQ	---	NQ	---	NQ	---	NQ	---	50.4	6%	46.8	7%	128.6	3%	123.4	4%
Gly	ND	---	NQ	---	ND	---	ND	---	NQ	---	NQ	---	NQ	---	NQ	---	NQ	---	NQ	---	9.6	4%	10.7	7%
Asp	3.7	5%	3.9	18%	1.4	7%	NQ	---	1.4	3%	NQ	---	NQ	---	NQ	---	183.8	4%	177.8	5%	693.2	3%	675.3	2%
Glu	NQ	---	ND	---	NQ	---	NQ	---	NQ	---	NQ	---	NQ	---	NQ	---	176.1	3%	172.6	6%	3306.5	1%	3413.9	3%
Thr	NQ	---	NQ	---	ND	---	ND	---	NQ	---	NQ	---	NQ	---	NQ	---	23.8	4%	23.1	10%	130.7	7%	129.6	7%
β-Ala	Not possible to be quantified.																							
α-Ala	--	--	3.2	16	--	--	NQ	---	NQ	---	2.2	6%	NQ	---	2.0	7%	NQ	---	85.5	9%	NQ	---	39.0	8%
GABA	NQ	---	NQ	---	ND	---	ND	---	0.9	1%	0.9	5%	0.8	1%	0.7	9%	54.4	13%	53.9	8%	709.4	1%	693.7	3%
Pro	5.7	2%	5.5	6%	8.5	1%	8.3	2%	8.8	2%	8.6	1%	8.3	1%	8.0	2%	31.8	3%	29.8	7%	31.5	16%	33.6	2%
Tyr	0.9	1%	1.1	20%	ND	---	ND	---	1.5	1%	1.3	12%	1.4	1%	1.2	13%	6.8	3%	8.7	12%	20.0	3%	21.8	11%
Val	2.5	8%	2.5	6%	NQ	---	NQ	---	1.6	2%	1.9	1%	1.6	7%	1.8	1%	27.3	4%	26.1	7%	21.3	14%	21.8	7%
Met	NQ	---	NQ	---	ND	---	NQ	---	NQ	---	NQ	---	NQ	---	NQ	---	6.6	2%	7.2	12%	8.0	3%	8.8	3%
Leu	2.5	0.3%	2.4	5%	NQ	---	NQ	---	3.1	5%	3.1	2%	2.9	1%	3.0	7%	16.7	4%	15.2	13%	26.2	8%	24.8	13%
Ile	1.5	3%	1.6	6%	ND	---	NQ	---	1.2	9%	1.3	4%	1.1	2%	1.1	8%	39.4	9%	40.8	8%	36.1	9%	37.7	2%
Trp	ND	---	ND	---	ND	---	ND	---	ND	---	NQ	---	ND	---	NQ	---	34.3	10%	35.5	6%	10.5	1%	10.4	3%
Phe	1.6	1%	1.7	8%	NQ	---	NQ	---	1.9	1%	2.0	1%	1.9	3%	1.9	2%	65.3	4%	64.0	6%	111.5	5%	111.5	2%
Orn	ND	---	ND	---	ND	---	ND	---	ND	---	ND	---	ND	---	ND	---	NQ	---	NQ	---	ND	---	ND	---
Lys	ND	---	ND	---	ND	---	ND	---	NQ	---	NQ	---	NQ	---	NQ	---	21.0	2%	21.1	9%	58.7	5%	58.2	8%

[E] For His, Arg, Asn, Asp, Glu, α-Ala, Trp, and Phe, n = 15; Gly, n = 5; Met, n = 6; and Orn n = 3.

[F] For His, Arg, Asn, Asp, Glu, Thr, α-Ala, Trp, and Phe, n = 15; Gly, n = 5; Met, n = 6; and Orn n = 5.

[G] For Asn, Thr, Phe, n = 12; Ser, Glu, Val, Leu, n = 6; Gly, Tyr, Met, Trp, n = 3.

[H] For Asn, Thr, Phe, n = 12; Ser, Glu, α-Ala, Val, Leu n = 6; Gly, Tyr, Met, Trp, n = 3.

ND: not detectable; NQ: Not quantifiable.

5. SUMMARY

Derivatization of analytes is one way to improve their retention in the stationary phase of reversed-phase liquid chromatography, and it also helps to increase their ionization efficiency, which ultimately leads to obtain better and more reliable results. In the present study, three derivatization reagents, DEEMM, AzoB, and AzoC, were evaluated for the determination of free amino acids in different matrices.

The work focused on the determination of derivatized analytes using an electrospray ion source (ESI) in negative ionization mode. The results were compared with the ESI in positive mode, which has been predominantly used so far. Although in negative ion mode, signals have a lower intensity, it was shown that the use of negative mode transitions also provides very similar results in terms of the limit of detection (LoD) compared to the positive mode. In some cases, the LoD values in the negative mode were even lower than in the positive mode. Although matrix effects affect both polarities, the negative mode was less affected by matrix effects. In the negative ionization mode, depending on the derivatization reagent, the fragmentation patterns can be influenced by the structure of the amino acid as it was shown for DEEMM and AzoC derivatives.

The possibility of using transitions in the negative ion mode to confirm the identity of the analytes when a quantitative transition was recorded in the positive mode was investigated. The method was tested by analyzing the amino acid content of different beverages and it was found that this approach meets the requirements set by both the SANTE/11312/2021 and 2021/808 guidelines.

From the studied derivatization reagents, AzoB showed to be the best option for non-targeted (derivatization targeted) analysis, since it can distinguish amino compounds from other types of analytes. It can go even one step further by differentiating amino acids from other amino compounds based on their fragmentation patterns.

6. REFERENCES

[1] "50 years of HPLC," *C&EN Global Enterp*, vol. 94, no. 24, pp. 28–33, Jun. 2016, doi: 10.1021/cen-09424-cover1.

[2] J. Buie, "Evolution of HPLC systems," vol. 5, no. 5, pp. 66–67, Jun. 2010.

[3] M. Yamashita and J. B. Fenn, "Electrospray ion source. Another variation on the free-jet theme," *J. Phys. Chem.*, vol. 88, no. 20, pp. 4451–4459, Sep. 1984, doi: 10.1021/j150664a002.

[4] A. H. Soeriyadi, M. R.Whittaker, C. Boyer, and T. P. Davis, "Soft ionization mass spectroscopy: Insights into the polymerization mechanism," *Journal of Polymer Science Part A: Polymer Chemistry*, vol. 51, no. 7, pp. 1475–1505, 2013, doi:10. 1002/pola.26536.

[5] A. Garcia-Ac, P. A. Segura, L. Viglino, C. Gagnon, and S. Sauvé, "Comparison of APPI, APCI and ESI for the LC-MS/MS analysis of bezafibrate, cyclophosphamide, enalapril, methotrexate and orlistat in municipal wastewater," *Journal of Mass Spectrometry*, vol. 46, no. 4, pp. 383–390, 2011, doi: 10.1002/jms.1904.

[6] M. E. Bier, "Coupling ESI and MALDI Sources to the Quadrupole Mass Filter, Quadrupole Ion Trap, Linear Quadrupole Ion Trap, and Orbitrap Mass Analyzers," in *Electrospray and MALDI Mass Spectrometry*, R. B. Cole, Ed., Hoboken, NJ, USA: John Wiley & Sons, Inc., 2012, pp. 263–344. doi: 10.1002/ 9780470588901.ch9.

[7] E. Boonstra, R. de Kleijn, L. S. Colzato, A. Alkemade, B. U. Forstmann, and S. Nieuwenhuis, "Neurotransmitters as food supplements: the effects of GABA on brain and behavior," *Front Psychol*, vol. 6, p. 1520, Oct. 2015, doi: 10.3389/fpsyg. 2015.01520.

[8] T. Okura *et al.*, "Hyperhomocysteinemia is one of the risk factors associated with cerebrovascular stiffness in hypertensive patients, especially elderly males," *Sci Rep*, vol. 4, no. 1, Art. no. 1, Jul. 2014, doi: 10.1038/srep05663.

[9] O. Nygård, J. E. Nordrehaug, H. Refsum, P. M. Ueland, M. Farstad, and S. E. Vollset, "Plasma Homocysteine Levels and Mortality in Patients with Coronary Artery Disease," *New England Journal of Medicine*, vol. 337, no. 4, pp. 230–237, Jul. 1997, doi: 10.1056/NEJM199707243370403.

[10] S. S. Rehr, D. H. Janzen, and P. P. Feeny, "L-Dopa in Legume Seeds: A Chemical Barrier to Insect Attack," *Science*, vol. 181, no. 4094, pp. 81–82, Jul. 1973, doi: 10.1126/science.181.4094.81.

[11] G. A. Rosenthal, "l-Canavanine: a higher plant insecticidal allelochemical," *Amino Acids*, vol. 21, no. 3, pp. 319–330, Nov. 2001, doi: 10.1007/s007260170017.

[12] A. Tilborg, B. Norberg, and J. Wouters, "Pharmaceutical salts and cocrystals involving amino acids: A brief structural overview of the state-of-art," *European Journal of Medicinal Chemistry*, vol. 74, pp. 411–426, Mar. 2014, doi: 10.1016/j. ejmech.2013.11.045.

[13] T. Sou, L. M. Kaminskas, T.-H. Nguyen, R. Carlberg, M. P. McIntosh, and D. A. V. Morton, "The effect of amino acid excipients on morphology and solid-state properties of multi-component spray-dried formulations for pulmonary delivery of biomacromolecules," *European Journal of Pharmaceutics and Biopharmaceutics*, vol. 83, no. 2, pp. 234–243, Feb. 2013, doi: 10.1016/j.ejpb.2012.10.015.

[14] I. Manoli and C. P. Venditti, "Disorders of branched chain amino acid metabolism," *Transl Sci Rare Dis*, vol. 1, no. 2, pp. 91–110, doi: 10.3233/TRD-160009.

[15] J. Löliger, “Function and Importance of Glutamate for Savory Foods,” *The Journal of Nutrition*, vol. 130, no. 4, pp. S915–S920, Apr. 2000, doi: 10.1093/jn/130.4.915S.
[16] E. A. Wistaff, S. Beller, A. Schmid, J. J. Neville, and T. Nietner, “Chemometric analysis of amino acid profiles for detection of fruit juice adulterations – Application to verify authenticity of blood orange juice,” *Food Chemistry*, vol. 343, p. 128452, May 2021, doi: 10.1016/j.foodchem.2020.128452.
[17] E. H. Soufleros, E. Bouloumpasi, C. Tsarchopoulos, and C. G. Biliaderis, “Primary amino acid profiles of Greek white wines and their use in classification according to variety, origin and vintage,” *Food Chemistry*, vol. 80, no. 2, pp. 261–273, Feb. 2003, doi: 10.1016/S0308-8146(02)00271-6.
[18] I. Hermosín, R. M. Chicón, and M. Dolores Cabezudo, “Free amino acid composition and botanical origin of honey,” *Food Chemistry*, vol. 83, no. 2, pp. 263–268, Nov. 2003, doi: 10.1016/S0308-8146(03)00089-X.
[19] M. Ohtani, M. Sugita, and K. Maruyama, “Amino Acid Mixture Improves Training Efficiency in Athletes,” *The Journal of Nutrition*, vol. 136, no. 2, pp. 538S-543S, Feb. 2006, doi: 10.1093/jn/136.2.538S.
[20] M. Williams, “Dietary Supplements and Sports Performance: Amino Acids,” *Journal of the International Society of Sports Nutrition*, vol. 2, no. 2, p. 63, Dec. 2005, doi: 10.1186/1550-2783-2-2-63.
[21] A. Gornischeff, J. Liigand, and R. Rebane, “A systematic approach toward comparing electrospray ionization efficiencies of derivatized and non-derivatized amino acids and biogenic amines,” *Journal of Mass Spectrometry*, vol. 53, no. 10, pp. 997–1004, 2018, doi: 10.1002/jms.4272.
[22] T. Yokoyama, M. Tokuda, M. Amano, and K. Mikami, “Simultaneous determination of primary and secondary d- and l-amino acids by reversed-phase high-performance liquid chromatography using pre-column derivatization with two-step labelling method,” *Bioscience, Biotechnology, and Biochemistry*, vol. 81, no. 9, pp. 1681–1686, Sep. 2017, doi: 10.1080/09168451.2017.1340090.
[23] M. Moulin, C. Deleu, F. R. Larher, and A. Bouchereau, “High-performance liquid chromatography determination of pipecolic acid after precolumn ninhydrin derivatization using domestic microwave,” *Analytical Biochemistry*, vol. 308, no. 2, pp. 320–327, Sep. 2002, doi: 10.1016/S0003-2697(02)00202-6.
[24] G. Zheng *et al.*, “A novel method for detecting amino acids derivatized with phenyl isothiocyanate by high-performance liquid chromatography–electrospray ionization mass spectrometry,” *International Journal of Mass Spectrometry*, vol. 392, pp. 1–6, Diciembre 2015, doi: 10.1016/j.ijms.2015.08.004.
[25] P. Kwanyuen and J. W. Burton, “A Modified Amino Acid Analysis Using PITC Derivatization for Soybeans with Accurate Determination of Cysteine and Half-Cystine,” *Journal of the American Oil Chemists’ Society*, vol. 87, no. 2, pp. 127–132, 2010, doi: 10.1007/s11746-009-1484-2.
[26] I. Kabelová, M. Dvořáková, H. Čížková, P. Dostálek, and K. Melzoch, “Determination of free amino acids in beers: A comparison of Czech and foreign brands,” *Journal of Food Composition and Analysis*, vol. 21, no. 8, pp. 736–741, Dec. 2008, doi: 10.1016/j.jfca.2008.06.007.
[27] Y.-S. Sung, A. Berthod, D. Roy, and D. W. Armstrong, “A Closer Examination of 6-Aminoquinolyl-N-Hydroxysuccinimidyl Carbamate Amino Acid Derivatization in HPLC with Multiple Detection Modes,” *Chromatographia*, vol. 84, no. 8, pp. 719–727, Aug. 2021, doi: 10.1007/s10337-021-04051-w.

[28] B. Redruello, V. Ladero, B. del Rio, M. Fernández, M. C. Martin, and M. A. Alvarez, "A UHPLC method for the simultaneous analysis of biogenic amines, amino acids and ammonium ions in beer," *Food Chemistry*, vol. 217, pp. 117–124, Feb. 2017, doi: 10.1016/j.foodchem.2016.08.040.
[29] R. Rebane and K. Herodes, "A sensitive method for free amino acids analysis by liquid chromatography with ultraviolet and mass spectrometric detection using precolumn derivatization with diethyl ethoxymethylenemalonate: Application to the honey analysis," *Analytica Chimica Acta*, vol. 672, no. 1, pp. 79–84, Jul. 2010, doi: 10.1016/j.aca.2010.04.014.
[30] Y. Tapuhi, D. E. Schmidt, W. Lindner, and B. L. Karger, "Dansylation of amino acids for high-performance liquid chromatography analysis," *Analytical Biochemistry*, vol. 115, no. 1, pp. 123–129, Jul. 1981, doi: 10.1016/0003-2697(81)90534-0.
[31] H.-L. Cai, R.-H. Zhu, and H.-D. Li, "Determination of dansylated monoamine and amino acid neurotransmitters and their metabolites in human plasma by liquid chromatography–electrospray ionization tandem mass spectrometry," *Analytical Biochemistry*, vol. 396, no. 1, pp. 103–111, Jan. 2010, doi: 10.1016/j.ab.2009.09.015.
[32] E. de J. Zapata Flores, K. Herodes, and I. Leito, "Comparison of the ionisation mode in the determination of free amino acids in beers by Liquid Chromatography tandem mass spectrometry," *Journal of Chromatography A*, vol. 1677, p. 463320, Aug. 2022, doi: 10.1016/j.chroma.2022.463320.
[33] Marc. Roth, "Fluorescence reaction for amino acids," *Anal. Chem.*, vol. 43, no. 7, pp. 880–882, Jun. 1971, doi: 10.1021/ac60302a020.
[34] J. D. H. Cooper, G. Ogden, J. McIntosh, and D. C. Turnell, "The stability of the o-phthalaldehyde/2-mercaptoethanol derivatives of amino acids: An investigation using high-pressure liquid chromatography with a precolumn derivatization technique," *Analytical Biochemistry*, vol. 142, no. 1, pp. 98–102, Oct. 1984, doi: 10.1016/0003-2697(84)90522-0.
[35] M. Friedman, "Applications of the Ninhydrin Reaction for Analysis of Amino Acids, Peptides, and Proteins to Agricultural and Biomedical Sciences," *J. Agric. Food Chem.*, vol. 52, no. 3, pp. 385–406, Feb. 2004, doi: 10.1021/jf030490p.
[36] R. Naffa, G. Holmes, W. Zhang, C. Maidment, I. Shehadi, and G. Norris, "Comparison of liquid chromatography with fluorescence detection to liquid chromatography-mass spectrometry for amino acid analysis with derivatisation by 6-aminoquinolyl-N-hydroxysuccinimidyl-carbamate: Applications for analysis of amino acids in skin," *Arabian Journal of Chemistry*, vol. 13, no. 2, pp. 3997–4008, Feb. 2020, doi: 10.1016/j.arabjc.2019.05.002.
[37] K. Shimbo, A. Yahashi, K. Hirayama, M. Nakazawa, and H. Miyano, "Multifunctional and Highly Sensitive Precolumn Reagents for Amino Acids in Liquid Chromatography/Tandem Mass Spectrometry," *Anal. Chem.*, vol. 81, no. 13, pp. 5172–5179, Jul. 2009, doi: 10.1021/ac900470w.
[38] N. Arashida, R. Nishimoto, M. Harada, K. Shimbo, and N. Yamada, "Highly sensitive quantification for human plasma-targeted metabolomics using an amine derivatization reagent," *Analytica Chimica Acta*, vol. 954, pp. 77–87, Feb. 2017, doi: 10.1016/j.aca.2016.11.068.
[39] S. Inagaki, Y. Tano, Y. Yamakata, T. Higashi, J. Z. Min, and T. Toyo'oka, "Highly sensitive and positively charged precolumn derivatization reagent for amines and amino acids in liquid chromatography/electrospray ionization tandem mass

spectrometry," *Rapid Communications in Mass Spectrometry*, vol. 24, no. 9, pp. 1358–1364, 2010, doi: 10.1002/rcm.4521.
[40] C. A. McNaney *et al.*, "Analysis of l-serine-O-phosphate in cerebrospinal spinal fluid by derivatization–liquid chromatography/mass spectrometry," *Analytical Biochemistry*, vol. 452, pp. 10–12, May 2014, doi: 10.1016/j.ab.2014.02.007.
[41] K. Shimbo, T. Oonuki, A. Yahashi, K. Hirayama, and H. Miyano, "Precolumn derivatization reagents for high-speed analysis of amines and amino acids in biological fluid using liquid chromatography/electrospray ionization tandem mass spectrometry," *Rapid Communications in Mass Spectrometry*, vol. 23, no. 10, pp. 1483–1492, 2009, doi: 10.1002/rcm.4026.
[42] R. Rebane, T. Rodima, A. Kütt, and K. Herodes, "Development of amino acid derivatization reagents for liquid chromatography electrospray ionization mass spectrometric analysis and ionization efficiency measurements," *Journal of Chromatography A*, vol. 1390, pp. 62–70, Apr. 2015, doi: 10.1016/j.chroma.2015.02.050.
[43] C. Ghosh, C. P. Shinde, and B. S. Chakraborty, "Ionization Polarity as a Cause of Matrix Effects, its Removal and Estimation in ESI-LC-MS/MS Bio-analysis," *J Anal Bioanal Techniques*, vol. 01, no. 02, 2010, doi: 10.4172/2155-9872.1000106.
[44] R. George, A. Haywood, S. Khan, M. Radovanovic, J. Simmonds, and R. Norris, "Enhancement and Suppression of Ionization in Drug Analysis Using HPLC-MS/MS in Support of Therapeutic Drug Monitoring: A Review of Current Knowledge of Its Minimization and Assessment," *Therapeutic Drug Monitoring*, vol. 40, no. 1, p. 1, Feb. 2018, doi: 10.1097/FTD.0000000000000471.
[45] B. K. Matuszewski, M. L. Constanzer, and C. M. Chavez-Eng, "Strategies for the Assessment of Matrix Effect in Quantitative Bioanalytical Methods Based on HPLC−MS/MS," *Anal. Chem.*, vol. 75, no. 13, pp. 3019–3030, Jul. 2003, doi: 10.1021/ac020361s.
[46] P. J. Taylor, "Matrix effects: the Achilles heel of quantitative high-performance liquid chromatography–electrospray–tandem mass spectrometry," *Clinical Biochemistry*, vol. 38, no. 4, pp. 328–334, Apr. 2005, doi: 10.1016/j.clinbiochem.2004.11.007.
[47] S. Gao, Z.-P. Zhang, and H. T. Karnes, "Sensitivity enhancement in liquid chromatography/atmospheric pressure ionization mass spectrometry using derivatization and mobile phase additives," *Journal of Chromatography B*, vol. 825, no. 2, pp. 98–110, Oct. 2005, doi: 10.1016/j.jchromb.2005.04.021.
[48] J. Ziegler and S. Abel, "Analysis of amino acids by HPLC/electrospray negative ion tandem mass spectrometry using 9-fluorenylmethoxycarbonyl chloride (Fmoc-Cl) derivatization," *Amino Acids*, vol. 46, no. 12, pp. 2799–2808, Dec. 2014, doi: 10.1007/s00726-014-1837-5.
[49] N. B. Cech and C. G. Enke, "Selectivity in Electrospray Ionization Mass Spectrometry," in *Electrospray and MALDI Mass Spectrometry*, R. B. Cole, Ed., Hoboken, NJ, USA: John Wiley & Sons, Inc., 2012, pp. 49–73. doi: 10.1002/9780470588901.ch2.
[50] H. Trufelli, P. Palma, G. Famiglini, and A. Cappiello, "An overview of matrix effects in liquid chromatography–mass spectrometry," *Mass Spectrometry Reviews*, vol. 30, no. 3, pp. 491–509, 2011, doi: 10.1002/mas.20298.
[51] J.-P. Antignac, K. de Wasch, F. Monteau, H. De Brabander, F. Andre, and B. Le Bizec, "The ion suppression phenomenon in liquid chromatography–mass spectro-

metry and its consequences in the field of residue analysis," *Analytica Chimica Acta*, vol. 529, no. 1, pp. 129–136, Jan. 2005, doi: 10.1016/j.aca.2004.08.055.
[52] S. Uekusa *et al.*, "Development of a Derivatization Reagent with a 2-Nitrophenylsulfonyl Moiety for UHPLC-HRMS/MS and Its Application to Detect Amino Acids Including Taurine," *Molecules*, vol. 26, no. 12, Art. no. 12, Jan. 2021, doi: 10.3390/molecules26123498.
[53] D. J. Strydom, "Amino acid analysis using various carbamate reagents for precolumn derivatization," in *Techniques in Protein Chemistry*, Elsevier, 1996, pp. 331–339. doi: 10.1016/S1080-8914(96)80037-8.
[54] A. Archut *et al.*, "Azobenzene-Functionalized Cascade Molecules: Photoswitchable Supramolecular Systems," *Chemistry – A European Journal*, vol. 4, no. 4, pp. 699–706, 1998, doi: 10.1002/(SICI)1521-3765(19980416)4:4<699::AID-CHEM699>3.0.CO;2-9.
[55] A. Fissi, O. Pieroni, and F. Ciardelli, "Photoresponsive polymers: Azobenzene-containing poly(L-lysine)," *Biopolymers*, vol. 26, no. 12, pp. 1993–2007, Dec. 1987, doi: 10.1002/bip.360261203.
[56] "SANTE/11312/2021, Analytical Quality Control And Method Validation Procedures For Pesticide Residues Analysis In Food And Feed," Jan. 2021.
[57] "COMMISSION IMPLEMENTING REGULATION (EU) 2021/808 of 22 March 2021 on the performance of analytical methods for residues of pharmacologically active substances used in food-producing animals and on the interpretation of results as well as on the methods to be used for sampling and repealing Decisions 2002/657/EC and 98/179/EC," *Off. J. Eur. Commun.*, vol. 64, pp. 84–109, May 2021.
[58] M.-L. Oldekop, R. Rebane, and K. Herodes, "Dependence of matrix effect on ionization polarity during LC–ESI–MS analysis of derivatized amino acids in some natural samples," *Eur J Mass Spectrom (Chichester)*, vol. 23, no. 5, pp. 245–253, Oct. 2017, doi: 10.1177/1469066717711026.
[59] J. J. Rodríguez-Bencomo, P. Rigou, F. Mattivi, F. López, and A. Mehdi, "Removal of biogenic amines from wines by chemisorption on functionalized silica and effects on other wine components," *Sci Rep*, vol. 10, no. 1, Art. no. 1, Oct. 2020, doi: 10.1038/s41598-020-74287-3.
[60] K. Cai *et al.*, "Free amino acids, biogenic amines, and ammonium profiling in tobacco from different geographical origins using microwave-assisted extraction followed by ultra high performance liquid chromatography," *Journal of Separation Science*, vol. 40, no. 23, pp. 4571–4582, 2017, doi: 10.1002/jssc.201700608.
[61] M.-L. Oldekop, K. Herodes, and R. Rebane, "Study of the matrix effects and sample dilution influence on the LC–ESI–MS/MS analysis using four derivatization reagents," *Journal of Chromatography B*, vol. 967, pp. 147–155, Sep. 2014, doi: 10.1016/j.jchromb.2014.07.027.
[62] C. Salazar, J. M. Armenta, and V. Shulaev, "An UPLC-ESI-MS/MS Assay Using 6-Aminoquinolyl-N-Hydroxysuccinimidyl Carbamate Derivatization for Targeted Amino Acid Analysis: Application to Screening of Arabidopsis thaliana Mutants," *Metabolites*, vol. 2, no. 3, pp. 398–428, Jul. 2012, doi: 10.3390/metabo2030398.
[63] N. Gray *et al.*, "High-Speed Quantitative UPLC-MS Analysis of Multiple Amines in Human Plasma and Serum via Precolumn Derivatization with 6-Aminoquinolyl-N-hydroxysuccinimidyl Carbamate: Application to Acetaminophen-Induced Liver Failure," *Anal. Chem.*, vol. 89, no. 4, pp. 2478–2487, Feb. 2017, doi: 10.1021/acs.analchem.6b04623.

[64] B. A. Boughton *et al.*, “Comprehensive Profiling and Quantitation of Amine Group Containing Metabolites,” *Anal. Chem.*, vol. 83, no. 19, pp. 7523–7530, Oct. 2011, doi: 10.1021/ac201610x.
[65] S. Zalipsky, “Alkyl succinimidyl carbonates undergo Lossen rearrangement in basic buffers,” *Chem. Commun.*, no. 1, pp. 69–70, 1998, doi: 10.1039/a706713e.
[66] A. Isidro-Llobet, X. Just-Baringo, A. Ewenson, M. Álvarez, and F. Albericio, “Fmoc-2-mercaptobenzothiazole, for the introduction of the Fmoc moiety free of side-reactions,” *Biopolymers*, vol. 88, no. 5, pp. 733–737, 2007, doi: 10.1002/bip.20732.
[67] B. L. M. Rao, S. Nowshuddin, A. Jha, M. K. Divi, and M. N. A. Rao, “Fmoc-OASUD: A new reagent for the preparation of Fmoc-amino acids free from impurities resulting from Lossen rearrangement,” *Tetrahedron Letters*, vol. 57, no. 37, pp. 4220–4223, Sep. 2016, doi: 10.1016/j.tetlet.2016.08.015.
[68] M. K. Hargreaves, J. G. Pritchard, and H. R. Dave, “Cyclic carboxylic monoimides,” *Chem. Rev.*, vol. 70, no. 4, pp. 439–469, Aug. 1970, doi: 10.1021/cr60266a001.
[69] L. A. Shemchuk, “ChemInform Abstract: Alkaline Hydrolysis and Alcoholysis of N-(2-Succinimidobenzamido)succinimide and N-(2-Glutarimidobenzamido)glutarimide.,” *ChemInform*, vol. 31, no. 37, 2000, doi: 10.1002/chin.200037045.
[70] A. R. Katritzky, J. Yao, M. Qi, Y. Chou, D. J. Sikora, and S. Davis, “Ring Opening Reactions of Succinimides,” *HETEROCYCLES*, vol. 48, no. 12, p. 2677, 1998, doi: 10.3987/REV-98-506.
[71] N. B. Cech and C. G. Enke, “Practical implications of some recent studies in electrospray ionization fundamentals,” *Mass Spectrometry Reviews*, vol. 20, no. 6, pp. 362–387, 2001, doi: 10.1002/mas.10008.
[72] M. Oss *et al.*, “Quantitative electrospray ionization efficiency scale: 10 years after,” *Rapid Communications in Mass Spectrometry*, vol. 35, no. 21, p. e9178, 2021, doi: 10.1002/rcm.9178.
[73] T. Nishimura and H. Kato, “Taste of free amino acids and peptides,” *Food Reviews International*, vol. 4, no. 2, pp. 175–194, Jan. 1988, doi: 10.1080/87559128809540828.
[74] A. Laffitte, F. Neiers, and L. Briand, “Characterization of taste compounds: chemical structures and sensory properties,” in *Flavour*, E. Guichard, C. Salles, M. Morzel, and A.-M. Le Bon, Eds., Chichester, UK: John Wiley & Sons, Ltd, 2016, pp. 154–191. doi: 10.1002/9781118929384.ch7.
[75] M. Fontana and S. Buiatti, “Amino Acids in Beer,” in *Beer in Health and Disease Prevention*, Elsevier, 2009, pp. 273–284. doi: 10.1016/B978-0-12-373891-2.00025-0.
[76] “Chemical and physical properties of beer,” in *Brewing*, Elsevier, 2004, pp. 662–715. doi: 10.1533/9781855739062.662.

SUMMARY IN ESTONIAN

Derivatiseerivad reagendid negatiivse režiimi elektropihustuse LC-MS analüüsil

Analüütide derivatiseerimine on üks võimalus nende retentsiooni parandamiseks pöördfaas-vedelikkromatograafia statsionaarses faasis, samuti aitab see suurendada analüütide ionisatsiooniefektiivsust, mis kokkuvõttes viib paremate ja usaldusväärsemate tulemusteni. Käesolevas uuringus hinnati kolme derivatiseerimisreaktiivi, DEEMM, AzoB ja AzoC, vabade aminohapete määramiseks erinevates maatriksites.

Töös keskenduti derivatiseeritud analüütide määramisele kasutades elektropihustuse ioonallikat (ESI) negatiivsete ioonide režiimis. Tulemusi võrreldi seni valdavalt kasutatava positiivsete ioonide ESI režiimiga. Kuigi negatiivsete ioonide režiimis on signaalid madalama intensiivsusega, näidati, et negatiivse režiimi üleminekute kasutamine annab positiivse režiimiga võrreldes väga sarnaseid tulemusi ka avastamispiiri (LoD) osas. Mõnel juhul olid negatiivse režiimi LoD väärtused isegi madalamad kui positiivses režiimis. Kuigi maatriksiefektid mõjutavad ioniseerumist mõlema polaarsuse korral, oli negatiivne režiim maatriksiefektidest vähem mõjutatud. Negatiivsete ioonide režiimis võib sõltuvalt derivatiseerimisreagendist fragmenteerumismustreid mõjutada aminohappe struktuur nagu seda näidati DEEMM-i ja AzoC derivaatide puhul.

Uuriti võimalust kasutada negatiivsete ioonide režiimi üleminekuid analüütide samasuse kinnitamiseks, kui kvantitatiivne üleminek oli registreeritud positiivses režiimis. Meetodit testiti erinevate jookide aminohappete sisalduse analüüsimisel ja leiti, et see lähenemisviis vastab nii SANTE/11312/2021 kui ka 2021/808 suunistega kehtestatud nõuetele.

Uuritud derivatiseerimisreagentidest pakkus AzoB Parimat võimalust aminoühendite mitte-sihitud (derivatiseerimine-sihitud) analüüsiks. See võimaldab tuvastada aminoühendeid suure hulga teiste ainete seast. Lisaks on AzoB-derivaatide fragmenteerumismustri abil võimalik eristada aminohappeid muudest amiinidest.

ACKNOWLEDGEMENTS

I must thank the University of Tartu and the Institute of Chemistry for allowing me to study in this wonderful place. My deepest gratitude to all professors that I have had during all these years in the PhD program at the University of Tartu. Especially, to my esteemed supervisors: Associated Professor Koit Herodes, for being an excellent, patient, and very nice mentor as well as to Professor Ivo Leito for all the help and advice you have provided me during this time.

My appreciation goes to my mother and my family who have always believed in me in every moment, thanks for their support and unconditional love. To my friends from Mexico: Carlos B., Chuy, Miriam, Mario, Evelin, Juan Carlos, Dalila, Sandra García, Oziel Loredo, Yessi, Cony, Tania, Roxana, Carmen, Amanda.

My life here in Estonia made me find a lot of friends, thanks to all of you: Ngan, for all the laughs we had, those moments I will always keep them in my heart, Duong, Kenneth, Jaypee, Yoab, Nikola, Asko, Rüta, Max, Larissa, Mari, Venusia, Sofja, and Tanya. Also, the friends I made by playing pokémon Go, Rafa, Martin, Marta, Ly, Helmi, Piret, Kaarel, Eva, etc.

To my teachers in Mexico, Norma G., Carmen V., Marco G., Perla C., Celinda M, Juana A, and Ernestina H. Special thanks to the Science and Technology Council of Mexico (Consejo Nacional de Ciencia y Tecnología, CONACYT) and the Science and Technology Council of San Luis Potosi (Consejo Potosino de Ciencia y Tecnología COPOCYT) that sponsored me during my studies (scholarship number 440655).

This work was supported by the Estonian Research Council grant PUT1589, by the EU through the European Regional Development Fund (TK141 “Advanced materials and high-technology devices for energy recuperation systems”) and was carried out using the instrumentation at the Estonian Center of Analytical Chemistry (www.akki.ee).

To all those people who were with me during all these wonderful years of my life.

SUUR AITÄH.

PUBLICATIONS

CURRICULUM VITAE

Name:	Ernesto de Jesus Zapata Flores
Born:	March 27, 1991, San Luis Potosi, Mexico.
Citizenship:	Mexican
E-mail:	ernesto.zapata@ut.ee

Education

2018–present	PhD student at Institute of Chemistry, University of Tartu.
2016–2018	Master of Science in Engineering, Applied Measurement Science, University of Tartu
2009–2015	Autonomous University of San Luis Potosi, B.Sc. (Chemistry).

Professional employment

2015–2016	Omega Chemicals S.A. de C.V, San Luis Potosi, Mexico (Chemist).

Scientific publications

1. **Zapata Flores, E. de J**.; Herodes, K.; Leito, I. Comparison of the Ionisation Mode in the Determination of Free Amino Acids in Beers by Liquid Chromatography Tandem Mass Spectrometry. *Journal of Chromatography A* **2022**, *1677*, 463320. https://doi.org/10.1016/j.chroma.2022.463320.
2. **Zapata Flores, E. de J**.; Bùi, N. K. N.; Selberg, S.; Herodes, K.; Leito, I. Comparison of Two Azobenzene-Based Amino Acid Derivatization Reagents for LC-MS/MS Analysis in Positive and Negative ESI Modes. *Talanta* **2023**, *252*, 123803. https://doi.org/10.1016/j.talanta.2022.123803.
3. **Zapata E,** Leito I, Herodes K. Positive + negative is not equal to zero: Use of negative ionisation as analyte identity confirmation tool in LC-ESI-MS analysis. European Journal of Mass Spectrometry. 2022;28(5-6):107-112. doi:10.1177/14690667221130160.
4. **Zapata-Flores, E.D.J., Gazcón-Orta, N.E., Flores-Vélez, L.M., 2016.** A direct method for the determination of lead in beers by differential pulse polarography-anodic stripping voltammetry. Journal of Materials and Environmental Science 7, 4467–4470.

Attended conferences

3rd Iberoamerican Conference on Mass Spectrometry in Rio de Janeiro (10-1.5.12.2022). Poster presentation.

ELULOOKIRJELDUS

Nimi: Ernesto de Jesus Zapata Flores
Sünniaeg: 27. märts 1991, San Luis Potosi, Mehhiko.
Kodakondsus: Mehhiko
E-post: ernesto.zapata@ut.ee

Hariduskäik

2018–present Tartu Ülikool, keemia doktorant.
2016–2018 Tartu Ülikool, Tehnikateaduse magister (rakenduslik mõõteteadus).
2009–2015 San Luis Potosi Autonoomne Ülikool, bakalauseuse kraad (Keemia).

Teenistuskäik

2015–2016 Omega Chemicals S.A. de C.V, San Luis Potosi, Mexico (Keemik).

Publikatsioone loetelu

1. **Zapata Flores, E. de J**.; Herodes, K.; Leito, I. Comparison of the Ionisation Mode in the Determination of Free Amino Acids in Beers by Liquid Chromatography Tandem Mass Spectrometry. *Journal of Chromatography A* **2022**, *1677*, 463320. https://doi.org/10.1016/j.chroma.2022.463320.
2. **Zapata Flores, E. de J**.; Bùi, N. K. N.; Selberg, S.; Herodes, K.; Leito, I. Comparison of Two Azobenzene-Based Amino Acid Derivatization Reagents for LC-MS/MS Analysis in Positive and Negative ESI Modes. *Talanta* **2023**, *252*, 123803. https://doi.org/10.1016/j.talanta.2022.123803.
3. **Zapata E,** Leito I, Herodes K. Positive + negative is not equal to zero: Use of negative ionisation as analyte identity confirmation tool in LC-ESI-MS analysis. European Journal of Mass Spectrometry. 2022;28(5-6):107-112. doi:10.1177/14690667221130160.
4. **Zapata-Flores, E.D.J., Gazcón-Orta, N.E., Flores-Vélez, L.M., 2016.** A direct method for the determination of lead in beers by differential pulse polarography-anodic stripping voltammetry. Journal of Materials and Environmental Science 7, 4467–4470.

Osalemine konverentsidel

3rd Iberoamerican Conference on Mass Spectrometry in Rio de Janeiro (10-1.5.12.2022). Stendiettekanne.

DISSERTATIONES CHIMICAE UNIVERSITATIS TARTUENSIS

1. **Toomas Tamm.** Quantum-chemical simulation of solvent effects. Tartu, 1993, 110 p.
2. **Peeter Burk.** Theoretical study of gas-phase acid-base equilibria. Tartu, 1994, 96 p.
3. **Victor Lobanov.** Quantitative structure-property relationships in large descriptor spaces. Tartu, 1995, 135 p.
4. **Vahur Mäemets.** The ^{17}O and ^{1}H nuclear magnetic resonance study of H_2O in individual solvents and its charged clusters in aqueous solutions of electrolytes. Tartu, 1997, 140 p.
5. **Andrus Metsala.** Microcanonical rate constant in nonequilibrium distribution of vibrational energy and in restricted intramolecular vibrational energy redistribution on the basis of slater's theory of unimolecular reactions. Tartu, 1997, 150 p.
6. **Uko Maran.** Quantum-mechanical study of potential energy surfaces in different environments. Tartu, 1997, 137 p.
7. **Alar Jänes.** Adsorption of organic compounds on antimony, bismuth and cadmium electrodes. Tartu, 1998, 219 p.
8. **Kaido Tammeveski.** Oxygen electroreduction on thin platinum films and the electrochemical detection of superoxide anion. Tartu, 1998, 139 p.
9. **Ivo Leito.** Studies of Brønsted acid-base equilibria in water and non-aqueous media. Tartu, 1998, 101 p.
10. **Jaan Leis.** Conformational dynamics and equilibria in amides. Tartu, 1998, 131 p.
11. **Toonika Rinken.** The modelling of amperometric biosensors based on oxidoreductases. Tartu, 2000, 108 p.
12. **Dmitri Panov.** Partially solvated Grignard reagents. Tartu, 2000, 64 p.
13. **Kaja Orupõld.** Treatment and analysis of phenolic wastewater with microorganisms. Tartu, 2000, 123 p.
14. **Jüri Ivask.** Ion Chromatographic determination of major anions and cations in polar ice core. Tartu, 2000, 85 p.
15. **Lauri Vares.** Stereoselective Synthesis of Tetrahydrofuran and Tetrahydropyran Derivatives by Use of Asymmetric Horner-Wadsworth-Emmons and Ring Closure Reactions. Tartu, 2000, 184 p.
16. **Martin Lepiku.** Kinetic aspects of dopamine D_2 receptor interactions with specific ligands. Tartu, 2000, 81 p.
17. **Katrin Sak.** Some aspects of ligand specificity of P2Y receptors. Tartu, 2000, 106 p.
18. **Vello Pällin.** The role of solvation in the formation of iotsitch complexes. Tartu, 2001, 95 p.
19. **Katrin Kollist.** Interactions between polycyclic aromatic compounds and humic substances. Tartu, 2001, 93 p.

20. **Ivar Koppel.** Quantum chemical study of acidity of strong and superstrong Brønsted acids. Tartu, 2001, 104 p.
21. **Viljar Pihl.** The study of the substituent and solvent effects on the acidity of OH and CH acids. Tartu, 2001, 132 p.
22. **Natalia Palm.** Specification of the minimum, sufficient and significant set of descriptors for general description of solvent effects. Tartu, 2001, 134 p.
23. **Sulev Sild.** QSPR/QSAR approaches for complex molecular systems. Tartu, 2001, 134 p.
24. **Ruslan Petrukhin.** Industrial applications of the quantitative structure-property relationships. Tartu, 2001, 162 p.
25. **Boris V. Rogovoy.** Synthesis of (benzotriazolyl)carboximidamides and their application in relations with *N*- and *S*-nucleophyles. Tartu, 2002, 84 p.
26. **Koit Herodes.** Solvent effects on UV-vis absorption spectra of some solvatochromic substances in binary solvent mixtures: the preferential solvation model. Tartu, 2002, 102 p.
27. **Anti Perkson.** Synthesis and characterisation of nanostructured carbon. Tartu, 2002, 152 p.
28. **Ivari Kaljurand.** Self-consistent acidity scales of neutral and cationic Brønsted acids in acetonitrile and tetrahydrofuran. Tartu, 2003, 108 p.
29. **Karmen Lust.** Adsorption of anions on bismuth single crystal electrodes. Tartu, 2003, 128 p.
30. **Mare Piirsalu.** Substituent, temperature and solvent effects on the alkaline hydrolysis of substituted phenyl and alkyl esters of benzoic acid. Tartu, 2003, 156 p.
31. **Meeri Sassian.** Reactions of partially solvated Grignard reagents. Tartu, 2003, 78 p.
32. **Tarmo Tamm.** Quantum chemical modelling of polypyrrole. Tartu, 2003. 100 p.
33. **Erik Teinemaa.** The environmental fate of the particulate matter and organic pollutants from an oil shale power plant. Tartu, 2003. 102 p.
34. **Jaana Tammiku-Taul.** Quantum chemical study of the properties of Grignard reagents. Tartu, 2003. 120 p.
35. **Andre Lomaka.** Biomedical applications of predictive computational chemistry. Tartu, 2003. 132 p.
36. **Kostyantyn Kirichenko.** Benzotriazole – Mediated Carbon–Carbon Bond Formation. Tartu, 2003. 132 p.
37. **Gunnar Nurk.** Adsorption kinetics of some organic compounds on bismuth single crystal electrodes. Tartu, 2003, 170 p.
38. **Mati Arulepp.** Electrochemical characteristics of porous carbon materials and electrical double layer capacitors. Tartu, 2003, 196 p.
39. **Dan Cornel Fara.** QSPR modeling of complexation and distribution of organic compounds. Tartu, 2004, 126 p.
40. **Riina Mahlapuu.** Signalling of galanin and amyloid precursor protein through adenylate cyclase. Tartu, 2004, 124 p.

41. **Mihkel Kerikmäe.** Some luminescent materials for dosimetric applications and physical research. Tartu, 2004, 143 p.
42. **Jaanus Kruusma.** Determination of some important trace metal ions in human blood. Tartu, 2004, 115 p.
43. **Urmas Johanson.** Investigations of the electrochemical properties of polypyrrole modified electrodes. Tartu, 2004, 91 p.
44. **Kaido Sillar.** Computational study of the acid sites in zeolite ZSM-5. Tartu, 2004, 80 p.
45. **Aldo Oras.** Kinetic aspects of dATPαS interaction with $P2Y_1$ receptor. Tartu, 2004, 75 p.
46. **Erik Mölder.** Measurement of the oxygen mass transfer through the air-water interface. Tartu, 2005, 73 p.
47. **Thomas Thomberg.** The kinetics of electroreduction of peroxodisulfate anion on cadmium (0001) single crystal electrode. Tartu, 2005, 95 p.
48. **Olavi Loog.** Aspects of condensations of carbonyl compounds and their imine analogues. Tartu, 2005, 83 p.
49. **Siim Salmar.** Effect of ultrasound on ester hydrolysis in aqueous ethanol. Tartu, 2006, 73 p.
50. **Ain Uustare.** Modulation of signal transduction of heptahelical receptors by other receptors and G proteins. Tartu, 2006, 121 p.
51. **Sergei Yurchenko.** Determination of some carcinogenic contaminants in food. Tartu, 2006, 143 p.
52. **Kaido Tämm.** QSPR modeling of some properties of organic compounds. Tartu, 2006, 67 p.
53. **Olga Tšubrik.** New methods in the synthesis of multisubstituted hydrazines. Tartu. 2006, 183 p.
54. **Lilli Sooväli.** Spectrophotometric measurements and their uncertainty in chemical analysis and dissociation constant measurements. Tartu, 2006, 125 p.
55. **Eve Koort.** Uncertainty estimation of potentiometrically measured ph and pK_a values. Tartu, 2006, 139 p.
56. **Sergei Kopanchuk.** Regulation of ligand binding to melanocortin receptor subtypes. Tartu, 2006, 119 p.
57. **Silvar Kallip.** Surface structure of some bismuth and antimony single crystal electrodes. Tartu, 2006, 107 p.
58. **Kristjan Saal.** Surface silanization and its application in biomolecule coupling. Tartu, 2006, 77 p.
59. **Tanel Tätte.** High viscosity $Sn(OBu)_4$ oligomeric concentrates and their applications in technology. Tartu, 2006, 91 p.
60. **Dimitar Atanasov Dobchev**. Robust QSAR methods for the prediction of properties from molecular structure. Tartu, 2006, 118 p.
61. **Hannes Hagu**. Impact of ultrasound on hydrophobic interactions in solutions. Tartu, 2007, 81 p.
62. **Rutha Jäger.** Electroreduction of peroxodisulfate anion on bismuth electrodes. Tartu, 2007, 142 p.

63. **Kaido Viht.** Immobilizable bisubstrate-analogue inhibitors of basophilic protein kinases: development and application in biosensors. Tartu, 2007, 88 p.
64. **Eva-Ingrid Rõõm.** Acid-base equilibria in nonpolar media. Tartu, 2007, 156 p.
65. **Sven Tamp.** DFT study of the cesium cation containing complexes relevant to the cesium cation binding by the humic acids. Tartu, 2007, 102 p.
66. **Jaak Nerut.** Electroreduction of hexacyanoferrate(III) anion on Cadmium (0001) single crystal electrode. Tartu, 2007, 180 p.
67. **Lauri Jalukse.** Measurement uncertainty estimation in amperometric dissolved oxygen concentration measurement. Tartu, 2007, 112 p.
68. **Aime Lust.** Charge state of dopants and ordered clusters formation in CaF_2:Mn and CaF_2:Eu luminophors. Tartu, 2007, 100 p.
69. **Iiris Kahn**. Quantitative Structure-Activity Relationships of environmentally relevant properties. Tartu, 2007, 98 p.
70. **Mari Reinik.** Nitrates, nitrites, N-nitrosamines and polycyclic aromatic hydrocarbons in food: analytical methods, occurrence and dietary intake. Tartu, 2007, 172 p.
71. **Heili Kasuk.** Thermodynamic parameters and adsorption kinetics of organic compounds forming the compact adsorption layer at Bi single crystal electrodes. Tartu, 2007, 212 p.
72. **Erki Enkvist.** Synthesis of adenosine-peptide conjugates for biological applications. Tartu, 2007, 114 p.
73. **Svetoslav Hristov Slavov**. Biomedical applications of the QSAR approach. Tartu, 2007, 146 p.
74. **Eneli Härk.** Electroreduction of complex cations on electrochemically polished Bi(*hkl*) single crystal electrodes. Tartu, 2008, 158 p.
75. **Priit Möller.** Electrochemical characteristics of some cathodes for medium temperature solid oxide fuel cells, synthesized by solid state reaction technique. Tartu, 2008, 90 p.
76. **Signe Viggor.** Impact of biochemical parameters of genetically different pseudomonads at the degradation of phenolic compounds. Tartu, 2008, 122 p.
77. **Ave Sarapuu.** Electrochemical reduction of oxygen on quinone-modified carbon electrodes and on thin films of platinum and gold. Tartu, 2008, 134 p.
78. **Agnes Kütt.** Studies of acid-base equilibria in non-aqueous media. Tartu, 2008, 198 p.
79. **Rouvim Kadis.** Evaluation of measurement uncertainty in analytical chemistry: related concepts and some points of misinterpretation. Tartu, 2008, 118 p.
80. **Valter Reedo.** Elaboration of IVB group metal oxide structures and their possible applications. Tartu, 2008, 98 p.
81. **Aleksei Kuznetsov.** Allosteric effects in reactions catalyzed by the cAMP-dependent protein kinase catalytic subunit. Tartu, 2009, 133 p.

82. **Aleksei Bredihhin.** Use of mono- and polyanions in the synthesis of multisubstituted hydrazine derivatives. Tartu, 2009, 105 p.
83. **Anu Ploom.** Quantitative structure-reactivity analysis in organosilicon chemistry. Tartu, 2009, 99 p.
84. **Argo Vonk.** Determination of adenosine A_{2A}- and dopamine D_1 receptor-specific modulation of adenylate cyclase activity in rat striatum. Tartu, 2009, 129 p.
85. **Indrek Kivi.** Synthesis and electrochemical characterization of porous cathode materials for intermediate temperature solid oxide fuel cells. Tartu, 2009, 177 p.
86. **Jaanus Eskusson.** Synthesis and characterisation of diamond-like carbon thin films prepared by pulsed laser deposition method. Tartu, 2009, 117 p.
87. **Marko Lätt.** Carbide derived microporous carbon and electrical double layer capacitors. Tartu, 2009, 107 p.
88. **Vladimir Stepanov.** Slow conformational changes in dopamine transporter interaction with its ligands. Tartu, 2009, 103 p.
89. **Aleksander Trummal.** Computational Study of Structural and Solvent Effects on Acidities of Some Brønsted Acids. Tartu, 2009, 103 p.
90. **Eerold Vellemäe.** Applications of mischmetal in organic synthesis. Tartu, 2009, 93 p.
91. **Sven Parkel.** Ligand binding to 5-HT_{1A} receptors and its regulation by Mg^{2+} and Mn^{2+}. Tartu, 2010, 99 p.
92. **Signe Vahur.** Expanding the possibilities of ATR-FT-IR spectroscopy in determination of inorganic pigments. Tartu, 2010, 184 p.
93. **Tavo Romann**. Preparation and surface modification of bismuth thin film, porous, and microelectrodes. Tartu, 2010, 155 p.
94. **Nadežda Aleksejeva.** Electrocatalytic reduction of oxygen on carbon nanotube-based nanocomposite materials. Tartu, 2010, 147 p.
95. **Marko Kullapere.** Electrochemical properties of glassy carbon, nickel and gold electrodes modified with aryl groups. Tartu, 2010, 233 p.
96. **Liis Siinor.** Adsorption kinetics of ions at Bi single crystal planes from aqueous electrolyte solutions and room-temperature ionic liquids. Tartu, 2010, 101 p.
97. **Angela Vaasa.** Development of fluorescence-based kinetic and binding assays for characterization of protein kinases and their inhibitors. Tartu 2010, 101 p.
98. **Indrek Tulp.** Multivariate analysis of chemical and biological properties. Tartu 2010, 105 p.
99. **Aare Selberg.** Evaluation of environmental quality in Northern Estonia by the analysis of leachate. Tartu 2010, 117 p.
100. **Darja Lavõgina.** Development of protein kinase inhibitors based on adenosine analogue-oligoarginine conjugates. Tartu 2010, 248 p.
101. **Laura Herm.** Biochemistry of dopamine D_2 receptors and its association with motivated behaviour. Tartu 2010, 156 p.

102. **Terje Raudsepp.** Influence of dopant anions on the electrochemical properties of polypyrrole films. Tartu 2010, 112 p.
103. **Margus Marandi.** Electroformation of Polypyrrole Films: *In-situ* AFM and STM Study. Tartu 2011, 116 p.
104. **Kairi Kivirand.** Diamine oxidase-based biosensors: construction and working principles. Tartu, 2011, 140 p.
105. **Anneli Kruve.** Matrix effects in liquid-chromatography electrospray mass-spectrometry. Tartu, 2011, 156 p.
106. **Gary Urb.** Assessment of environmental impact of oil shale fly ash from PF and CFB combustion. Tartu, 2011, 108 p.
107. **Nikita Oskolkov.** A novel strategy for peptide-mediated cellular delivery and induction of endosomal escape. Tartu, 2011, 106 p.
108. **Dana Martin.** The QSPR/QSAR approach for the prediction of properties of fullerene derivatives. Tartu, 2011, 98 p.
109. **Säde Viirlaid.** Novel glutathione analogues and their antioxidant activity. Tartu, 2011, 106 p.
110. **Ülis Sõukand.** Simultaneous adsorption of Cd^{2+}, Ni^{2+}, and Pb^{2+} on peat. Tartu, 2011, 124 p.
111. **Lauri Lipping.** The acidity of strong and superstrong Brønsted acids, an outreach for the "limits of growth": a quantum chemical study. Tartu, 2011, 124 p.
112. **Heisi Kurig.** Electrical double-layer capacitors based on ionic liquids as electrolytes. Tartu, 2011, 146 p.
113. **Marje Kasari.** Bisubstrate luminescent probes, optical sensors and affinity adsorbents for measurement of active protein kinases in biological samples. Tartu, 2012, 126 p.
114. **Kalev Takkis.** Virtual screening of chemical databases for bioactive molecules. Tartu, 2012, 122 p.
115. **Ksenija Kisseljova**. Synthesis of aza-β^3-amino acid containing peptides and kinetic study of their phosphorylation by protein kinase A. Tartu, 2012, 104 p.
116. **Riin Rebane.** Advanced method development strategy for derivatization LC/ESI/MS. Tartu, 2012, 184 p.
117. **Vladislav Ivaništšev.** Double layer structure and adsorption kinetics of ions at metal electrodes in room temperature ionic liquids. Tartu, 2012, 128 p.
118. **Irja Helm.** High accuracy gravimetric Winkler method for determination of dissolved oxygen. Tartu, 2012, 139 p.
119. **Karin Kipper.** Fluoroalcohols as Components of LC-ESI-MS Eluents: Usage and Applications. Tartu, 2012, 164 p.
120. **Arno Ratas.** Energy storage and transfer in dosimetric luminescent materials. Tartu, 2012, 163 p.
121. **Reet Reinart-Okugbeni**. Assay systems for characterisation of subtype-selective binding and functional activity of ligands on dopamine receptors. Tartu, 2012, 159 p.

122. **Lauri Sikk.** Computational study of the Sonogashira cross-coupling reaction. Tartu, 2012, 81 p.
123. **Karita Raudkivi.** Neurochemical studies on inter-individual differences in affect-related behaviour of the laboratory rat. Tartu, 2012, 161 p.
124. **Indrek Saar.** Design of GalR2 subtype specific ligands: their role in depression-like behavior and feeding regulation. Tartu, 2013, 126 p.
125. **Ann Laheäär.** Electrochemical characterization of alkali metal salt based non-aqueous electrolytes for supercapacitors. Tartu, 2013, 127 p.
126. **Kerli Tõnurist.** Influence of electrospun separator materials properties on electrochemical performance of electrical double-layer capacitors. Tartu, 2013, 147 p.
127. **Kaija Põhako-Esko.** Novel organic and inorganic ionogels: preparation and characterization. Tartu, 2013, 124 p.
128. **Ivar Kruusenberg.** Electroreduction of oxygen on carbon nanomaterial-based catalysts. Tartu, 2013, 191 p.
129. **Sander Piiskop.** Kinetic effects of ultrasound in aqueous acetonitrile solutions. Tartu, 2013, 95 p.
130. **Ilona Faustova**. Regulatory role of L-type pyruvate kinase N-terminal domain. Tartu, 2013, 109 p.
131. **Kadi Tamm.** Synthesis and characterization of the micro-mesoporous anode materials and testing of the medium temperature solid oxide fuel cell single cells. Tartu, 2013, 138 p.
132. **Iva Bozhidarova Stoyanova-Slavova.** Validation of QSAR/QSPR for regulatory purposes. Tartu, 2013, 109 p.
133. **Vitali Grozovski**. Adsorption of organic molecules at single crystal electrodes studied by *in situ* STM method. Tartu, 2014, 146 p.
134. **Santa Veikšina**. Development of assay systems for characterisation of ligand binding properties to melanocortin 4 receptors. Tartu, 2014, 151 p.
135. **Jüri Liiv.** PVDF (polyvinylidene difluoride) as material for active element of twisting-ball displays. Tartu, 2014, 111 p.
136. **Kersti Vaarmets.** Electrochemical and physical characterization of pristine and activated molybdenum carbide-derived carbon electrodes for the oxygen electroreduction reaction. Tartu, 2014, 131 p.
137. **Lauri Tõntson**. Regulation of G-protein subtypes by receptors, guanine nucleotides and Mn^{2+}. Tartu, 2014, 105 p.
138. **Aiko Adamson.** Properties of amine-boranes and phosphorus analogues in the gas phase. Tartu, 2014, 78 p.
139. **Elo Kibena**. Electrochemical grafting of glassy carbon, gold, highly oriented pyrolytic graphite and chemical vapour deposition-grown graphene electrodes by diazonium reduction method. Tartu, 2014, 184 p.
140. **Teemu Näykki.** Novel Tools for Water Quality Monitoring – From Field to Laboratory. Tartu, 2014, 202 p.
141. **Karl Kaupmees.** Acidity and basicity in non-aqueous media: importance of solvent properties and purity. Tartu, 2014, 128 p.

142. **Oleg Lebedev**. Hydrazine polyanions: different strategies in the synthesis of heterocycles. Tartu, 2015, 118 p.
143. **Geven Piir.** Environmental risk assessment of chemicals using QSAR methods. Tartu, 2015, 123 p.
144. **Olga Mazina.** Development and application of the biosensor assay for measurements of cyclic adenosine monophosphate in studies of G protein-coupled receptor signalinga. Tartu, 2015, 116 p.
145. **Sandip Ashokrao Kadam.** Anion receptors: synthesis and accurate binding measurements. Tartu, 2015, 116 p.
146. **Indrek Tallo.** Synthesis and characterization of new micro-mesoporous carbide derived carbon materials for high energy and power density electrical double layer capacitors. Tartu, 2015, 148 p.
147. **Heiki Erikson.** Electrochemical reduction of oxygen on nanostructured palladium and gold catalysts. Tartu, 2015, 204 p.
148. **Erik Anderson.** *In situ* Scanning Tunnelling Microscopy studies of the interfacial structure between Bi(111) electrode and a room temperature ionic liquid. Tartu, 2015, 118 p.
149. **Girinath G. Pillai.** Computational Modelling of Diverse Chemical, Biochemical and Biomedical Properties. Tartu, 2015, 140 p.
150. **Piret Pikma.** Interfacial structure and adsorption of organic compounds at Cd(0001) and Sb(111) electrodes from ionic liquid and aqueous electrolytes: an *in situ* STM study. Tartu, 2015, 126 p.
151. **Ganesh babu Manoharan.** Combining chemical and genetic approaches for photoluminescence assays of protein kinases. Tartu, 2016, 126 p.
152. **Carolin Siimenson**. Electrochemical characterization of halide ion adsorption from liquid mixtures at Bi(111) and pyrolytic graphite electrode surface. Tartu, 2016, 110 p.
153. **Asko Laaniste.** Comparison and optimisation of novel mass spectrometry ionisation sources. Tartu, 2016, 156 p.
154. **Hanno Evard.** Estimating limit of detection for mass spectrometric analysis methods. Tartu, 2016, 224 p.
155. **Kadri Ligi.** Characterization and application of protein kinase-responsive organic probes with triplet-singlet energy transfer. Tartu, 2016, 122 p.
156. **Margarita Kagan.** Biosensing penicillins' residues in milk flows. Tartu, 2016, 130 p.
157. **Marie Kriisa.** Development of protein kinase-responsive photoluminescent probes and cellular regulators of protein phosphorylation. Tartu, 2016, 106 p.
158. **Mihkel Vestli.** Ultrasonic spray pyrolysis deposited electrolyte layers for intermediate temperature solid oxide fuel cells. Tartu, 2016, 156 p.
159. **Silver Sepp**. Influence of porosity of the carbide-derived carbon on the properties of the composite electrocatalysts and characteristics of polymer electrolyte fuel cells. Tartu, 2016, 137 p.
160. **Kristjan Haav**. Quantitative relative equilibrium constant measurements in supramolecular chemistry. Tartu, 2017, 158 p.

161. **Anu Teearu**. Development of MALDI-FT-ICR-MS methodology for the analysis of resinous materials. Tartu, 2017, 205 p.
162. **Taavi Ivan**. Bifunctional inhibitors and photoluminescent probes for studies on protein complexes. Tartu, 2017, 140 p.
163. **Maarja-Liisa Oldekop**. Characterization of amino acid derivatization reagents for LC-MS analysis. Tartu, 2017, 147 p.
164. **Kristel Jukk**. Electrochemical reduction of oxygen on platinum- and palladium-based nanocatalysts. Tartu, 2017, 250 p.
165. **Siim Kukk**. Kinetic aspects of interaction between dopamine transporter and *N*-substituted nortropane derivatives. Tartu, 2017, 107 p.
166. **Birgit Viira**. Design and modelling in early drug development in targeting HIV-1 reverse transcriptase and Malaria. Tartu, 2017, 172 p.
167. **Rait Kivi**. Allostery in cAMP dependent protein kinase catalytic subunit. Tartu, 2017, 115 p.
168. **Agnes Heering**. Experimental realization and applications of the unified acidity scale. Tartu, 2017, 123 p.
169. **Delia Juronen**. Biosensing system for the rapid multiplex detection of mastitis-causing pathogens in milk. Tartu, 2018, 85 p.
170. **Hedi Rahnel.** ARC-inhibitors: from reliable biochemical assays to regulators of physiology of cells. Tartu, 2018, 176 p.
171. **Anton Ruzanov.** Computational investigation of the electrical double layer at metal–aqueous solution and metal–ionic liquid interfaces. Tartu, 2018, 129 p.
172. **Katrin Kestav.** Crystal Structure-Guided Development of Bisubstrate-Analogue Inhibitors of Mitotic Protein Kinase Haspin. Tartu, 2018, 166 p.
173. **Mihkel Ilisson.** Synthesis of novel heterocyclic hydrazine derivatives and their conjugates. Tartu, 2018, 101 p.
174. **Anni Allikalt.** Development of assay systems for studying ligand binding to dopamine receptors. Tartu, 2018, 160 p.
175. **Ove Oll.** Electrical double layer structure and energy storage characteristics of ionic liquid based capacitors. Tartu, 2018, 187 p.
176. **Rasmus Palm.** Carbon materials for energy storage applications. Tartu, 2018, 114 p.
177. **Jörgen Metsik.** Preparation and stability of poly(3,4-ethylenedioxythiophene) thin films for transparent electrode applications. Tartu, 2018, 111 p.
178. **Sofja Tšepelevitš.** Experimental studies and modeling of solute-solvent interactions. Tartu, 2018, 109 p.
179. **Märt Lõkov.** Basicity of some nitrogen, phosphorus and carbon bases in acetonitrile. Tartu, 2018, 104 p.
180. **Anton Mastitski**. Preparation of α-aza-amino acid precursors and related compounds by novel methods of reductive one-pot alkylation and direct alkylation. Tartu, 2018, 155 p.
181. **Jürgen Vahter**. Development of bisubstrate inhibitors for protein kinase CK2. Tartu, 2019, 186 p.

182. **Piia Liigand.** Expanding and improving methodology and applications of ionization efficiency measurements. Tartu, 2019, 189 p.
183. **Sigrid Selberg.** Synthesis and properties of lipophilic phosphazene-based indicator molecules. Tartu, 2019, 74 p.
184. **Jaanus Liigand.** Standard substance free quantification for LC/ESI/MS analysis based on the predicted ionization efficiencies. Tartu, 2019, 254 p.
185. **Marek Mooste.** Surface and electrochemical characterisation of aryl film and nanocomposite material modified carbon and metal-based electrodes. Tartu, 2019, 304 p.
186. **Mare Oja.** Experimental investigation and modelling of pH profiles for effective membrane permeability of drug substances. Tartu, 2019, 306 p.
187. **Sajid Hussain.** Electrochemical reduction of oxygen on supported Pt catalysts. Tartu, 2019, 220 p.
188. **Ronald Väli.** Glucose-derived hard carbon electrode materials for sodium-ion batteries. Tartu, 2019, 180 p.
189. **Ester Tee.** Analysis and development of selective synthesis methods of hierarchical micro- and mesoporous carbons. Tartu, 2019, 210 p.
190. **Martin Maide.** Influence of the microstructure and chemical composition of the fuel electrode on the electrochemical performance of reversible solid oxide fuel cell. Tartu, 2020, 144 p.
191. **Edith Viirlaid.** Biosensing Pesticides in Water Samples. Tartu, 2020, 102 p.
192. **Maike Käärik.** Nanoporous carbon: the controlled nanostructure, and structure-property relationships. Tartu, 2020, 162 p.
193. **Artur Gornischeff.** Study of ionization efficiencies for derivatized compounds in LC/ESI/MS and their application for targeted analysis. Tartu, 2020, 124 p.
194. **Reet Link.** Ligand binding, allosteric modulation and constitutive activity of melanocortin-4 receptors. Tartu, 2020, 108 p.
195. **Pilleriin Peets.** Development of instrumental methods for the analysis of textile fibres and dyes. Tartu, 2020, 150 p.
196. **Larisa Ivanova.** Design of active compounds against neurodegenerative diseases. Tartu, 2020, 152 p.
197. **Meelis Härmas.** Impact of activated carbon microstructure and porosity on electrochemical performance of electrical double-layer capacitors. Tartu, 2020, 122 p.
198. **Ruta Hecht.** Novel Eluent Additives for LC-MS Based Bioanalytical Methods. Tartu, 2020, 202 p.
199. **Max Hecht.** Advances in the Development of a Point-of-Care Mass Spectrometer Test. Tartu, 2020, 168 p.
200. **Ida Rahu.** Bromine formation in inorganic bromide/nitrate mixtures and its application for oxidative aromatic bromination. Tartu, 2020, 116 p.
201. **Sander Ratso**. Electrocatalysis of oxygen reduction on non-precious metal catalysts. Tartu, 2020, 371 p.
202. **Astrid Darnell.** Computational design of anion receptors and evaluation of host-guest binding. Tartu, 2021, 150 p.

203. **Ove Korjus.** The development of ceramic fuel electrode for solid oxide cells. Tartu, 2021, 150 p.
204. **Merit Oss.** Ionization efficiency in electrospray ionization source and its relations to compounds' physico-chemical properties. Tartu, 2021, 124 p.
205. **Madis Lüsi**. Electroreduction of oxygen on nanostructured palladium catalysts. Tartu, 2021, 180 p.
206. **Eliise Tammekivi.** Derivatization and quantitative gas-chromatographic analysis of oils. Tartu, 2021, 122 p.
207. **Simona Selberg.** Development of Small-Molecule Regulators of Epi-transcriptomic Processes. Tartu, 2021, 122 p.
208. **Olivier Etebe Nonga.** Inhibitors and photoluminescent probes for in vitro studies on protein kinases PKA and PIM. Tartu, 2021, 189 p.
209. **Riinu Härmas.** The structure and H2 diffusion in porous carbide-derived carbon particles. Tartu, 2022, 123 p.
210. **Maarja Paalo.** Synthesis and characterization of novel carbon electrodes for high power density electrochemical capacitors. Tartu, 2022, 144 p.
211. **Jinfeng Zhao.** Electrochemical characteristics of Bi(hkl) and micro-meso-porous carbon electrodes in ionic liquid based electrolytes. Tartu, 2022, 134 p.
212. **Alar Heinsaar.** Investigation of oxygen electrode materials for high-temperature solid oxide cells in natural conditions. Tartu, 2022, 120 p.
213. **Jaana Lilloja.** Transition metal and nitrogen doped nanocarbon cathode catalysts for anion exchange membrane fuel cells. Tartu, 2022, 202 p.
214. **Maris-Johanna Tahk.** Novel fluorescence-based methods for illuminating transmembrane signal transduction by G-protein coupled receptors. Tartu, 2022, 200 p.
215. **Eerik Jõgi.** Development and Applications of E. coli Immunosensor. Tartu, 2022, 103 p.
216. **Alo Rüütel.** Design principles of synthetic molecular receptors for anion-selective electrodes. Tartu, 2022, 109 p.
217. **Tanel Sõrmus.** Development of stimuli-responsive and covalent bisubstrate inhibitors of protein kinases. Tartu, 2022, 148 p.
218. **Oleg Artemchuk.** Autotrophic nitrogen removal processes for nutrient removal from sidestream and mainstream wastewater. Tartu, 2022, 115 p.
219. **Andre Leesment.** Quantitative studies of Brønsted acidity in biphasic systems and gas-phase. Tartu, 2023, 83 p.
220. **Meeli Arujõe-Sado.** Structural effects in aza-peptide bond formation reaction. Tartu, 2023, 83 p.
221. **Jonas Mart Linge.** Electrochemical reduction of oxygen on silver-based catalysts. Tartu, 2023, 269 p.
222. **Tõnis Laasfeld.** Integrating Image Analysis and Quantitative Modeling for a Holistic View of GPCR Ligand Binding Dynamics. Tartu, 2023, 226 p.